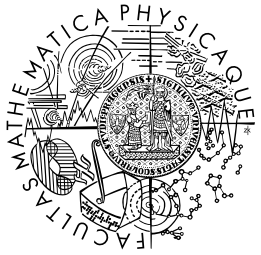

FACULTY
OF MATHEMATICS
AND PHYSICS
Charles University

DOCTORAL THESIS

Daniel Šimsa

Subtle effects in atoms and molecules

Department of Chemical Physics and Optics

Supervisor of the doctoral thesis:	doc. Mgr. Jaroslav Zamastil, Ph.D.
Study programme:	Physics
Study branch:	Biophysics, Chemical and Macromolecular Physics

Prague 2018

I declare that I carried out this doctoral thesis independently, and only with the cited sources, literature and other professional sources.

I understand that my work relates to the rights and obligations under the Act No. 121/2000 Sb., the Copyright Act, as amended, in particular the fact that the Charles University has the right to conclude a license agreement on the use of this work as a school work pursuant to Section 60 subsection 1 of the Copyright Act.

In ..... date ..... signature of the author

Title: Subtle effects in atoms and molecules

Author: Daniel Šimsa

Department: Department of Chemical Physics and Optics

Supervisor: doc. Mgr. Jaroslav Zamastil, Ph.D., Department of Chemical Physics and Optics

Abstract: The thesis is divided into two parts. The first part deals with radiative corrections in muonic hydrogen. The effect of vacuum polarization is studied, and the simplified derivation of the Wichmann-Kroll potential is presented. The energy shift caused by vacuum polarization to the Lamb shift in muonic hydrogen is calculated and it agrees with results in literature. Further, the concept of the extended Bethe logarithm is introduced and its advantages are shown and used to calculate the combined self-energy vacuum polarization contribution to the Lamb shift in muonic hydrogen. The results given here are more accurate and somewhat different from others given in literature. In the second part, the ground-state energy splitting due to the tunneling in a two-dimensional double-well potential is calculated. A systematic WKB expansion of the energy splitting is given. An interplay between curvature of the classical tunneling path and quantum nature of motion is observed. A series is found that describes systems with strong coupling like the proton transfer in malonaldehyde. The results show a strong sensitivity of the splitting on slight variations of the parameters entering the Hamiltonian linearly. This indicates a presence of quantum chaos in this problem.

Keywords: radiative corrections, vacuum polarization, tunneling, WKB approximation

I thank my supervisor doc. Mgr. Jaroslav Zamastil, Ph.D. for an interesting topic, stimulating leadership and his frank and unreserved attitude. I am grateful to my parents J. and M. Šimsovi for their neverending support and to my siblings for their encouragement. Above all, I would like to express my gratitude to my girlfriend M. Zámečníková for her kind understanding and all-round help, especially for carefully reading the manuscript.

Contents

Introduction

Small discrepancies between a theory and an experiment can turn out to be the motivation for a development of new theories. As a prime example one may mention perihelion precession of Mercury, which helped A. Einstein to establish a general theory of relativity.

One of the systems where subtle effects can be studied and which also served many times as an inspiration for new theories is the hydrogen atom. For example, the Bohr model, which explains the Rydberg formula for atomic atomic hydrogen-emission lines, was one of the foundation stones of quantum theory. Studying subtle features, however, provides even more information. The Dirac equation was validated by explaining fine details of hydrogen spectrum and later the measurement of the small energy difference between $2S_{1/2}$ and $2P_{1/2}$ states, called the Lamb shift, was the stimulus for a development of modern quantum electrodynamics (QED) [26]. Nowadays, testing QED on hydrogen-like atoms still raises some questions of crucial importance, like the size and structure of the proton.

These subtle effects that are still not fully understood can be found not only in atoms, but also in molecules. One of such effects is multi-dimensional tunneling. Although tunneling is well understood in systems that are described by one-dimensional potentials, the nonseparable multi-dimensional potentials still pose a problem. Among such systems are molecules like malonaldehyde, where a proton tunnels through a two-dimensional barrier.

In the first chapter we give a brief and concise theory description of both electronic and muonic hydrogen-like atoms and then we discuss in detail QED processes we have studied. In the second chapter we discuss the tunneling in two-dimensional potentials and we introduce a new method that can be used to calculate the energy splitting caused by tunneling. In Conclusion we summarize the results and we outline possible continuation of this work.

1. Radiative Corrections in Muonic Hydrogen

1.1 Motivation

Few years back, the $1S-2S$ transition in atomic hydrogen (e^-p^+) was determined to be

$$\nu_{1S-2S} = 2466061413187035(10) \quad \text{Hz}, \tag{1.1}$$

i.e. with relative uncertainty of 4.2×10^{-15} [19]. If we want to achieve such an extraordinary precision in theoretical predictions, we have to include even subtle effects like finite size of the nucleus, relativistic or radiative corrections originating from QED. Unfortunately, the proton charge radius[1] r_p is not known with sufficient precision. However, we can change our perspective and treat the value r_p as an adjustable parameter and use both experimental and theoretical results in atomic hydrogen to extract the value of the proton charge radius [18]

$$r_p = (0.8759 \pm 0.0077)\,\text{fm}. \tag{1.2}$$

Combining these and scattering experiment results we get the CODATA value [18]

$$r_p = (0.8751 \pm 0.0061)\,\text{fm}. \tag{1.3}$$

The value (1.3) was widely accepted until 2010, when a paper [22] was published and a discrepancy was reported therein. The authors measured a transition frequency between $2S_{1/2}\,(F=1)$ and $2P_{3/2}\,(F=2)$ states in muonic hydrogen (μ^-p^+)

$$E_{exp} = (206.2949 \pm 0.0032)\,\text{meV}. \tag{1.4}$$

This result is not as precise as (1.1), but the muon is approximately 200 times heavier than electron, thus, it is much more sensitive to the size of the proton. According to Standard Model (SM), the interaction Lagrangian between either electron e^- or muon μ^- and proton p^+ is the same with the only difference of having a different mass. The theoretical prediction of the transitional frequency (1.4) gives[2]

$$E_{exp} = (209.9974 \pm 0.0048 - 5.2262\frac{r_p^2}{\text{fm}^2})\,\text{meV}. \tag{1.5}$$

One can compare experimental (1.4) and theoretical (1.5) results and obtain the proton radius [13]

$$r_p = (0.84169 \pm 0.00066)\,\text{fm}. \tag{1.6}$$

The disagreement between (1.2) and (1.6) is 4.5σ and between (1.3) and (1.6) it is even 5.6σ [13], where σ is the standard deviation. Similar discrepancy has been established between deuterium (e^-d^+) and muonic deuterium (μ^-d^+) [23]. What might be the problem?

[1] It is correctly called bound-state root-mean square charge radius of the proton and is defined as $r_p^2 = \int \mathrm{d}^3\mathbf{r}\, r^2 \rho_p(\mathbf{r})$, where $\rho_p(\mathbf{r})$ is the charge density distribution of the proton.

[2] We keep the units usually used in literature, i.e. Hz for electron hydrogen and meV for muonic hydrogen.

1. **An error in the experiments**. The error in the muonic hydrogen spectroscopy experiment seems unlikely. It is both more sensitive to the r_p and more straightforward than hydrogen spectroscopy. Further, a new experiment was conducted [1] and the disagreement persists. On the other hand, some concerns were raised about the evaluation of hydrogen spectroscopy and electron-proton scattering experiments [2]. The value of Rydberg constant $R_\infty c$ has to be taken from other transitions than $1S - 2S$ and then plugged into the calculations. Even a small change on the order of uncertainty in some of those transitions may explain the puzzle. Others [27] question the statistics and the process of extraction of r_p value from scattering experiments. New experiments that can address these concerns are either under way or in the process of preparation [2].

2. **An error in the theoretical calculation** of corrections either for electronic or muonic hydrogen. The determination of the corrections is often complicated and we cannot discard the possibility that some mistakes or incorrect aproximations were made. Although many corrections were recalculated [13, 34] some have not been independently checked.

3. **A fundamental problem with SM**. Might this be a glimpse at a completely new physics? If the previously mentioned attempts to explain the puzzle are not successful we might consider the possibility that we are detecting physics beyond SM.

In this work we aim to recalculate some corrections relevant for muonic hydrogen and we check the values reported in literature [18, 9, 13, 30]. We study the Wichmann-Kroll term [30], which has not been independently derived so far. We also study the two-photon self-energy vacuum polarization correction which was firstly calculated in [21] and then the value was reduced by 60 % in [13].

1.2 Overview of theory of muonic and electronic hydrogen

The hydrogen-like atom, either muonic or electonic, is an ideal system for testing the agreement between theory and experiment. The Schrödinger and Dirac equations can be solved analytically, hence the approximations to the theory are made only in the subsequent steps. When one starts with an approximate solution, as it is in the case of atoms and molecules containing two or more electrons, it is much more complicated to control the accuracy in the subsequent steps with more approximations.

1.2.1 Energy levels given by Schrödinger equation

Transitional frequencies ν_{ab} between states a and b are given by

$$\nu_{ab} = \frac{E_b - E_a}{h}, \tag{1.7}$$

where E_a, resp. E_b are energies of the states a, resp. b and h is the Planck constant.

The crudest estimate of the energy levels of hydrogen-like atoms with the charge number Z in state a is given by the eigenvalue of the Schrödinger equation [31]

$$E_a^{\mathrm{Schr}} = -\frac{m(Z\alpha)^2c^2}{2n_a^2}. \tag{1.8}$$

where α stands for the fine structure constant, c for the speed of light, n_a and n_b, are the principal quantum numbers of the states a and b. Finaly, m is the mass of the lighter particle – in our case either electron $m = m_e$ or muon $m = m_\mu$. The equation (1.8) is a good estimate which explains the three digits of the $1S - 2S$ transition (1.1) in hydrogen. We improve the estimate and explain another two digits of (1.1) if we treat the nucleus not as an infinitely heavy particle, but incoroporate the finite mass of the nucleus m_N into the relation (1.8). We do it easily, by replacing the mass m by the reduced mass

$$m_r = \frac{m\, m_N}{m + m_N} = \frac{m}{1 + \frac{m}{m_N}}\,. \tag{1.9}$$

This is a direct consequence of the fact that from the perspective of nonrelativistic theory, we can shift to the center-of-mass system and treat a two-particle problem as a problem of one particle with the mass m_r in the given potential.

If we calculate transition frequencies between states with different principal quantum numbers we always factor out the nonrelativistic estimate of the energy (1.8). This approach is widely used because Rydberg constant $R_\infty c$ can be measured with higher precision than electron mass, Planck constant and fine structure constant that are linked to the Rydberg constant through the relation

$$R_\infty c = \frac{m_e\alpha^2c^2}{2h}\,. \tag{1.10}$$

If we want to go beyond this level of accuracy and theoretically explain the remaining eleven digits in (1.1), we need to account for even more subtle effects.

In the following part of this section we give an overview of these effects. An extended introduction to the topic can be found in [9], an overview of the recent theoretical and experimental results is given in [18].

1.2.2 Classification of the corrections

The corrections are generated by the effects ignored in the Schrödinger equation. They are included by means of perturbation theory. These corrections are much smaller than the Schrödinger eigenvalue (1.8) so the utilization of perturbation approach is justified. Even better, the corretions can be classified by powers of small paramaters, most importantly α, $Z\alpha$ and m/m_N, which have their origin in electrodynamic corrections[3]. Other corrections of nonelectromagnetic origin, which are induced by the weak or strong interaction, give additional small parameters such as the Fermi constant or ratio of nuclear radius and either electronic or muonic Bohr radius. We note that the coefficients may be logarithmic functions

[3] In the text, we do not mix parameters $Z\alpha$ and α, although the magnitude is, at least for low Z, given by magnitude of α. This is because $Z\alpha$ originates from **binding** between particles whereas α comes from **QED loops**. We want to distinguish between those two cases.

of the small parameters. In most cases the magnitude of the corrections can be guessed from the power of the parameters. For example, a one-loop radiative correction proportional to $\alpha(Z\alpha)^5$ is approximately hundred times bigger than a two-loop correction proportional to $\alpha^2(Z\alpha)^5$.

The corrections have larger values for S states than for P, D and other states with nonzero angular momentum. This is due to the short-range nature of the QED and other effects. This can be seen from the leading order corrections that are proportional to the magnitude of a wave function in origin $|\psi(0)|^2 \propto \delta_{l0}/n^3$ which is nonzero only for S states.

Let us now classify the corrections according to the powers of the small parameters mentioned above.

- Corrections which depend only on the parameter $Z\alpha$ are called **relativistic corrections**. They arise from the deviation from nonrelativistic theory and include effects like relativistic dependence of mass on the velocity, spin-orbit interaction, etc. In the leading order they are proportional to $(Z\alpha)^4$.

- Corrections which depend on the parameters α and $Z\alpha$ are called **radiative corrections** and they come from QED. The power of α is exactly equal to the number of electromagnetic loops. Among these corrections are effects like electron self-energy or vacuum polarization. They start to contribute at the order $\alpha(Z\alpha)^4$.

- Corrections which depend on the parameters m/m_N and $Z\alpha$ are called **recoil corrections**[4]. They reflect the fact that the nucleus does not have an infinitely heavy mass. The most important part is reflected by the substitution of mass m by the reduced mass m_r in (1.8). The second most important recoil contribution is of order $(m/m_N)(Z\alpha)^4$.

- Mixing the last two corrections together we get the so called **radiative-recoil corrections**. They depend on parameters α, $Z\alpha$, m/m_N. We have to take into account both the electromagnetic loops and the relativistic two-body nature of the system.

- Lastly, we have **nonelectromagnetic corrections** which are induced by the strong and weak interaction. The most important of these corrections are associated with nonzero radius of the proton and its structure.

Before we start the calculation, let us discuss magnitude of energy level shifts and splittings caused by some corrections for both electronic and muonic hydrogen with emphasis on those which are the most relevant to the measured transitions, $1S - 2S$ for electronic hydrogen (1.1) and $2^3S_{1/2} - 2^5P_{3/2}$ for muonic hydrogen (1.4). The situation for electronic hydrogen is shown on Fig. 1.1. The most important are relativistic effects, which explain the fine structure (difference between $2P_{3/2}$ and $2P_{1/2}$). They are followed by QED effects, which give rise to the Lamb shift. Almost on the same scale is the hyperfine structure. The corrections given by nonzero proton charge radius r_p are much smaller, but for the precision achieved in (1.1) are still very much relevant.

[4] If the power of the parameter $(Z\alpha)^n$ is $n \geq 5$, they are sometimes called relativistic recoil corrections.

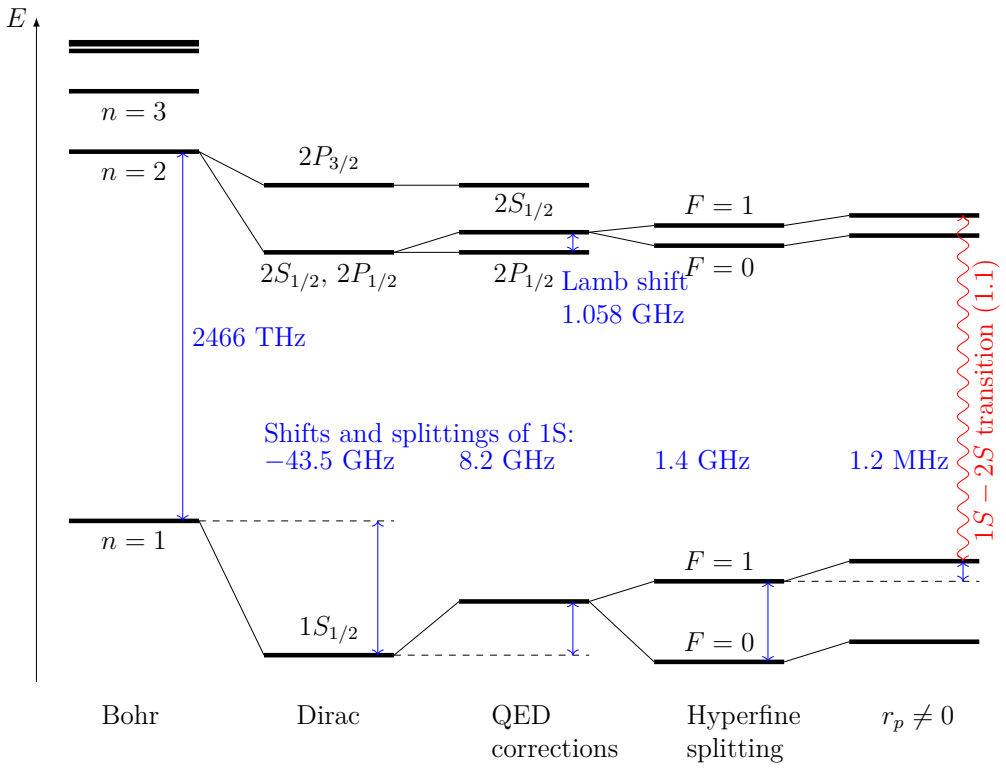

Figure 1.1: Several energy levels of hydrogen and their shifts and splittings caused by different effects.

For muonic hydrogen, the situation is not only quantitatively, but also qualitatively different, see Fig. 1.2. The $2S_{1/2}$ state lies lower than the $2P_{1/2}$ state. This is opposite in the electronic hydrogen, cf. differences between Figs. 1.1 and 1.2. Roughly speaking, this is given by the competition between vacuum polarization effect, which lowers the S states and is much stronger for muonic hydrogen, and self-energy effect, which increases the energy of S states and is relatively stronger for electronic hydrogen. Second difference in muonic hydrogen is that the fine structure splitting of $2P$ state is much smaller than the Lamb shift. This is given by the very strong vacuum polarization effect as well. It is much stronger not only than the self-energy but also relativistic corrections.

We can see from Fig. 1.2 that the transition $2^3S_{1/2} - 2^5P_{3/2}$ is a sum of three contributions:

1. $2S - 2P_{1/2}$ Lamb shift,
2. $2P_{1/2} - 2P_{3/2}$ fine structure splitting,
3. $2S$ and $2P_{3/2}$ hyperfine structure.

The effects studied by us are mostly relevant for the Lamb shift. An overview of the most important contributions to the Lamb shift in muonic hydrogen is given in Tab. 1.1.

In the next part of this chapter we first discuss some of the corrections from Tab. 1.1 and then we give a description of the corrections studied by us. We

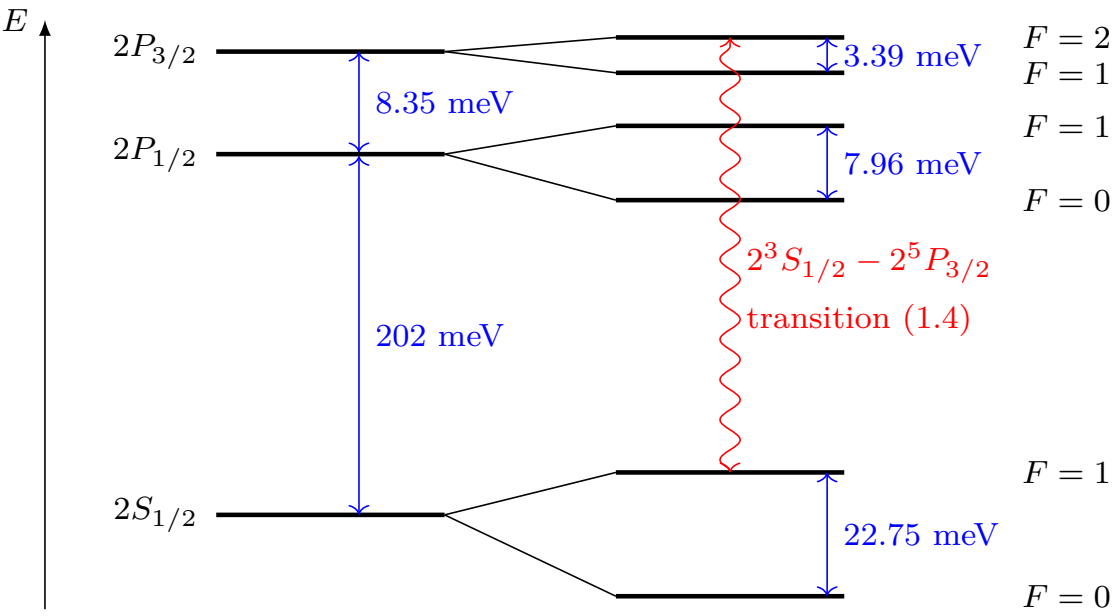

Figure 1.2: Structure of energy levels with $n = 2$ of muonic hydrogen.

present the derivation of the general formula and then we give the numeric results for the Lamb shift in muonic hydrogen.

1.2.3 Leading relativistic and recoil corrections

The analytic solution of the Dirac equation gives an energy eigenvalue of the system which consists of an electron bound in a Coulomb field created by a nucleus

$$E_D = mc^2 f\,(n, j)\,, \tag{1.11}$$

where, as usual, $j(j+1)$ is the eigenvalue of the total angular momenta $\hat{J}^2$ and function $f\,(n, j)$ is given by

$$f\,(n, j) = \frac{1}{\sqrt{1 + \frac{(Z\alpha)^2}{\left(n - j - \frac{1}{2} + \sqrt{j + \frac{1}{2} - (Z\alpha)^2}\right)^2}}}\,. \tag{1.12}$$

The equation (1.11) is valid only for an infinitely heavy nucleus. When we want to incorporate the finite nucleus mass m_N into the expression (1.11) the situation is not as straightforward as in the nonrelativistic case. On the other hand, the electron motion in the Coulomb field with low Z is substantially nonrelativistic; therefore, the binding energy should be proportional to the reduced mass m_r rather than just to the mass m. Considering this we can expect the equation in the form

$$E_D = m_r c^2 f\,(n, j)\,. \tag{1.13}$$

This might be a good first step but we need to go beyond that.

An unambiguous way to find energy levels of two-interacting-fermion problem is provided by the Bethe-Salpeter (BS) equation [24]. However, analytical solution of this equation is not known and calculations beyond the leading order is very complicated and nontransparent [3, 9].

#	Correction in [meV]	Value from [13, 22]	Uncert.	Our value
1	One-loop electron VP (Uehling)	205.0282		
2	Two-loop electron VP (Källen-Sabry)	1.5081		
3	Polarization insertion in two Coulomb lines	0.1509		
4	Three-loop electron VP	0.0076		
5	Polarization insertion in two and three Coulomb lines	0.00223		
6	Virtual Delbrück scattering	0.00014	±0.00002	
7	Wichmann-Kroll	−0.00103		−0.001016
8	Muon SE + VP	−0.6677		
9	Two-loop SEVP	−0.0025		−0.002706
10	Recoil correction (Darwin-Foldy term)	−0.0575		
11	Additional recoil	−0.04497		
12	Radiative-recoil	−0.00960		
13	Hadronic polarization	0.0108		
14	Nuclear structure correction (Proton polarizability)	0.015	±0.004	
	Sum of all r_p-independent corrections	209.9974	±0.0048	209.9972

Table 1.1: Example of some r_p-independent corrections to the Lamb shift in muonic hydrogen. Values in the third and fourth columns are taken from [13] and [22]. In the last column are our values. For the comparison, the r_p-dependent contribution is equal to 5.2262 $\frac{r_p^2}{\mathrm{fm}^2}$ meV.

A different and commonly used approach is based on the construction of an effective Hamiltonian which has both proper mass and relativistic dependence. It is called the Breit Hamiltonian and it is derived as a first order expansion in v^2/c^2 from a sum of free-particle relativistic Hamiltonians and the relativistic one-photon exchange which is of order $(Z\alpha)^4$ [3]. Extra photon exchange leads to at least one extra factor of $Z\alpha$, thus generating contributions to the energy of order $(Z\alpha)^5$ and higher [9]. Up to the order $(Z\alpha)^4$ we thus have

$$E_M = -\frac{m_r c^2 (Z\alpha)^2}{2n^2} - \frac{m_r c^2 (Z\alpha)^4}{2n^3}\left(\frac{1}{j+1/2} - \frac{3}{4n} + \frac{m_r}{4n(m+m_N)}\right) + \\ + \frac{m_r^3 c^2 (Z\alpha)^4}{m_N^2 2n^3}\left(\frac{1}{j+1/2} - \frac{1}{l+1/2}\right)(1-\delta_{l0}) \ , \quad (1.14)$$

where l is the nonrelativistic orbital angular momentum quantum number. The last term, which is nonzero only for states with $l > 0$ is called the Darwin-Foldy contribution.

Using the formula (1.14) we lose the exact treatment of the relativistic corrections embedded in (1.12). On the other hand, we get a practical recipe how

to treat the recoil corrections[5] which is not possible[6] from the completely relativistic approach (BS equation). Above that, we can calculate purely relativistic corrections to any order in $Z\alpha$ by simply expanding (1.12) in $Z\alpha$.

1.2.4 Self-energy

The most important radiative correction for electronic hydrogen comes from the so called self-energy (SE). According to QED an electron interacts with its own field, i.e. it continuously emits and reabsorbs virtual photons. This can be represented by a Feynman diagram on Fig. 1.3.

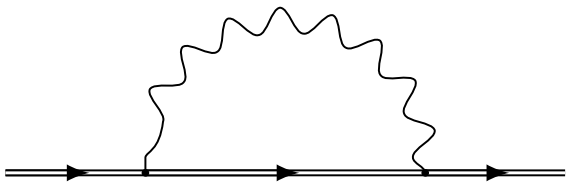

Figure 1.3: Feynman diagram of the one-photon self-energy

Using the Feynman rules [11, 26, 31], the diagram on Fig. 1.3 can be translated to an expression for the energy shift

$$\Delta E_{\mathrm{SE}} = \frac{\alpha}{\pi}\int \frac{\mathrm{d}^4 k_F}{k^2}\langle\psi_{\mathrm{at}}|\gamma_\mu \frac{1}{\gamma\cdot(\Pi-k)-m}\gamma_\mu|\psi_{\mathrm{at}}\rangle\,. \tag{1.15}$$

Here $\mathrm{d}^4k_F = i(2\pi)^{-2}\mathrm{d}^4k$, ψ_{at} is a wave function of a bound lepton, Π is the four-momentum of the lepton in an external Coulomb field $\Pi = \left(E+\frac{Z\alpha}{r},\mathbf{p}\right)$ and γ_μ are the Dirac matrices. It is customary to write the energy shift (1.15) in the form

$$\Delta E_{\mathrm{SE}} = \frac{\alpha}{\pi}(Z\alpha)^4\left(\frac{m_r}{m}\right)^3 F(Z\alpha)mc^2\,, \tag{1.16}$$

where $F(Z\alpha)$ is a dimensionless function

$$\begin{aligned} F(Z\alpha) = {} & A_{41}\ln(Z\alpha)^{-2} + A_{40} + A_{50}(Z\alpha) + \\ & + (Z\alpha)^2\left[A_{62}\ln^2(Z\alpha)^{-2} + A_{61}\ln(Z\alpha)^{-2} + G_{\mathrm{SE}}(Z\alpha)\right]. \end{aligned} \tag{1.17}$$

The remainder function $G_{\mathrm{SE}}(Z\alpha)$ can be calculated either from a further expansion in $Z\alpha$ or non-perturbatively. We have shown in [20] that for the perturbative expansion in $Z\alpha$ the structure of the remainder function $G_{\mathrm{SE}}(Z\alpha)$ is as follows

$$\begin{aligned} G_{\mathrm{SE}}(Z\alpha) = {} & A_{60} + (Z\alpha)\left[\ln(Z\alpha)^{-2}A_{71} + A_{70}\right] + \\ & + (Z\alpha)^2\left[\ln^3(Z\alpha)^{-2}A_{83} + \ln^2(Z\alpha)^{-2}A_{82} + \ln(Z\alpha)^{-2}A_{81} + A_{80}\right] + \\ & + (Z\alpha)^3\left[\ln^2(Z\alpha)^{-2}A_{92} + \ln(Z\alpha)^{-2}A_{91} + A_{90}\right] + \ldots\,. \end{aligned} \tag{1.18}$$

The coefficient A_{70} is not known, it is thus better to calculate the remainder function $G_{\mathrm{SE}}(Z\alpha)$ non-pertubatively (or expand it in a different way). The evaluation has been accomplished either by means of extrapolation of a partial wave

[5] As well as radiative-recoil corrections.

[6] At least, it is not known.

expansion (PWE) [12] or by means of relativistic generalization of multipole expansion (RME) [32, 33, 34]. In these works the energy splitting was determined with uncertainty less than 20 Hz. It is not enough to match the accuracy of the experiment but it is more than enough to independently confirm that the proton radius puzzle does not come from a mistake in evaluation of this correction.

1.2.5 Vacuum polarization

The Feynman diagram of one-loop VP is illustrated on Fig. 1.4.

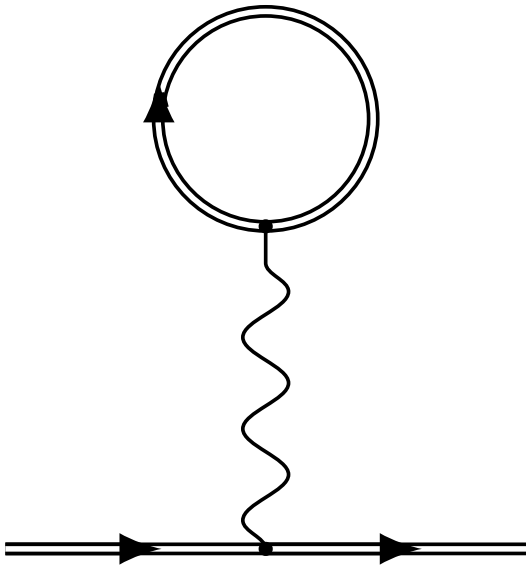

Figure 1.4: Feynman diagram of the one-loop vacuum polarization

The vacuum polarization level shift can be written as

$$E_{\mathrm{VP}} = \frac{\alpha}{\pi}\frac{(Z\alpha)^4}{n^3}\left(\frac{m_r}{m}\right)^3 H(Z\alpha)mc^2 \tag{1.19}$$

where $H(Z\alpha)$ is a dimensionless function of the form

$$H(Z\alpha) = H^{(1)}_{\mathrm{U}} + (Z\alpha)^2 H^{(3)}_{\mathrm{WK}} + \cdots . \tag{1.20}$$

The first term is due to the Uehling potential and the second is due to the Wichmann-Kroll potential. For electronic hydrogen these terms can be further expanded in $Z\alpha$, for muonic hydrogen such expansion is not valid. We postpone further discussion at this point because the vacuum polarization will be discussed in detail in Sec. 1.3.

1.2.6 Two-photon corrections

The two-photon corrections mean that two loops, either of SE or VP type, are combined. These corrections are at least α/π times smaller than the SE or VP effects alone. In the muonic hydrogen the third most important contribution is the two-loop VP, often called Källen-Sabry terms [14]. These effects were recalculated many times, for example in [13]. There are ten Feynman diagrams of two-photon corrections which subsets are referred to as SESE, SEVP and VPVP, depending

on which loops are combined. In this work we describe and calculate some of SEVP corrections in Sec. 1.4. Three-photon corrections are again at least α/π smaller than two-photon corrections.

1.2.7 Nuclear size and structure

The nucleus is a bound system of strongly interacting quarks. However, the quantum chromodynamics (QCD), a modern theory of strong interaction, is unable to provide us with tools which could be used to evaluate the corrections. The QCD perturbation expansion does not work on the distances relevant in atoms and non-perturbative methods are not well developed. Fortunately, the main nuclear parameters affecting the energy levels can be either measured directly or calculated from other experimental measurements.

The leading nuclear structure contribution gives the level shift

$$\Delta E^{(0)}_{\mathrm{NS}} = \mathcal{E}_{\mathrm{NS}}\delta_{l0}\,. \tag{1.21}$$

The leading order value $\mathcal{E}_{\mathrm{NS}}$ depends on the small parameters in the following way

$$\mathcal{E}_{\mathrm{NS}} = \frac{2}{3}\left(\frac{m_r}{m}\right)^3 \frac{(Z\alpha)^4}{n^3} mc^2 \frac{r_N^2}{\lambda\!\!\!^{-2}_C}\,, \tag{1.22}$$

where r_N is the nuclear charge radius and $\lambda\!\!\!^{-}_C$ is the Compton wavelength of the lepton divided by 2π. For an electron, the ratio $r_N/\lambda\!\!\!^{-}_C < 10^{-3}$ is indeed a small parameter, for a muon this ratio is only around 10^{-1} and thus the the nuclear size effect is the second strongest effect in the muonic hydrogen, see caption of Tab. 1.1.

As in the case of the level differences, we can add higher-order contributions which depent not only on small parameters such as α or $r_N/\lambda\!\!\!^{-}_C$ but also other constants that depend on other characteristics of the nucleus

$$\Delta E_{\mathrm{NS}} = \mathcal{E}_{\mathrm{NS}}(\delta_{l0} + \text{corrections})\,. \tag{1.23}$$

The corrections beyond the leading order link the size of the nucleus with the relativistic, radiative and other corrections [9].

An important correction is the nuclear polarizability which depends on electric and magnetic polarizabilities of the nucleus [9]. This correction inserts the highest uncertainty through the experimental error of polarizabilities [22].

Another important corrections depend on the so called third Zemach moment[7] $\langle r_N^3\rangle_{(2)}$. The relation between r_p and $\langle r_N^3\rangle_{(2)}$ can be derived. Unfortunately, it depends on the nuclear charge density which is not known [9]. On the other hand, the third Zemach radius can be obtained experimentally from scattering data in a model-independent way [13]. The disadvantage is that it inserts additional experimental uncertainty to the theoretical prediction (1.5).

Also a very small contribution is generated by exchange of a weak boson, but that can be ignored on present level of accuracy.

[7] Defined via convolution of two nuclear charge densities $\rho_N(\mathbf{r})$ as $\langle r_N^3\rangle_{(2)} = \int \mathrm{d}^3\mathbf{r}_1\,\mathrm{d}^3\mathbf{r}_2\,\rho_N(\mathbf{r}_1)\rho_N(\mathbf{r}_2)|\mathbf{r}_1+\mathbf{r}_2|^3$.

1.2.8 Hyperfine splitting

So far, we have completely ignored nuclear spin. It gives rise to additional energy level splitting which is usually called hyperfine splitting (HFS). Fortunately, it can be understood within the framework of nonrelativistic quantum mechanics. It originates from the interaction between magnetic moments of lepton and nucleus which are nonzero since their inner angular momentum, spin, is nonzero. The Hamiltonian is given by the analogy with classical electrodynamics. Magnetic dipole moment in the presence of a magnetic field has a form

$$\hat{H}_{\rm hfs} = -g_N \mu_N \hat{\mathbf{S}}_N \cdot \mathbf{B}, \tag{1.24}$$

where g_N is the nuclear g-factor, μ_N is nuclear magneton, $\hat{\mathbf{S}}_N$ is the spin of the nucleus and $\mathbf{B}$ is the magnetic field. For the splitting of $1S_{1/2}$ we get

$$\Delta E^{(0)}_{\rm hfs} = \mathcal{E}_{\rm hfs} = \frac{8}{3} g_N \left(Z\alpha\right)^4 \frac{m}{m_N} \left(\frac{m_r}{m}\right)^3 mc^2 \tag{1.25}$$

We can see that the energy splitting is suppressed by the factor $\left(Z\alpha\right)^2 m/m_N$ relatively to the Schrödinger value (1.8), therefore the perturbation treatment is justified. In order to get sufficient accuracy we again need to calculate numerous corrections to the hyperfine splitting (1.25).

$$\Delta E_{\rm hfs} = \mathcal{E}_{\rm hfs} \times (1 + \text{corrections}) \tag{1.26}$$

There are again the three small parameters α, $Z\alpha$ and m_e/m_N and a machinery of QED that can be employed to calculate these corrections, such as relativistic (binding), radiative, recoil, nuclear size and polarizability and other type of corrections discussed earlier. Among the radiative corrections, we also have the so called electron or muon **anomalous moment corrections** which are of the order $\alpha^n \mathcal{E}_{\rm hfs}$. These are the simplest radiative corrections because they are independent of the binding parameter $Z\alpha$ and they coincide with the anomalous moment of a free electron or muon.

1.3 Vacuum polarization in Coulomb field

The phenomenon of the vacuum polarization (VP) is caused by a photon that virtually decays into an electron-positron pair. In the vicinity of the nucleus the electron-positron pair is oriented as suggested on Fig. 1.5, and an induced charge distribution gives rise to an electrostatic potential which modifies the Coulomb field.

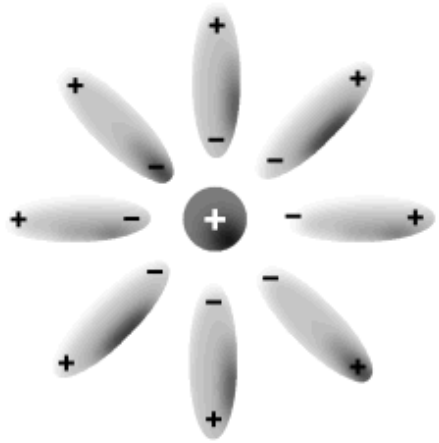

Figure 1.5: Illustration of a Vacuum polarization.

The Feynman diagram of one-loop VP has been shown in Fig. 1.4. Of course, the loop does not have to be electronic, i.e. the virtual decay can be into a different pair of leptons like muon-antimuon. For this reason we use $m_{\rm loop}$ for the mass of the virtual particle. In the subsequent calculation of the electronic VP, which is stronger than muonic or other VP, we insert to the formulae $m_{\rm loop} = m_e$. The treatment of hadronic VP is somewhat different, but it is also much weaker than electronic VP.

Evaluation of the influence of one-loop electronic VP in Coulomb field on the atomic energy levels in the leading order was accomplished long time ago by Uehling [29]. His result was recalculated many times and it is now included in many introductory texts to quantum field theory, for example [11, 26, 31]. On the other hand, calculation beyond the leading term was done by Wichmann and Kroll (WK) [30] and no independent derivation of their result has been made. In fact, Brown *et al.* [8] checked the $1/r$ part of the potential created by vacuum polarization. Wichmann and Kroll gave expression for the Laplace transform of the potential created by induced charge density. Their result was transformed to coordinate space by Blomqvist [6]. Recent evaluations of the influence of Wichmann and Kroll term on the energy levels of muonic hydrogen [7, 15] are based on approximations of the corresponding potential given in [9] which are in turn based on Blomqvist's work [6]. We also note that in this section we switch to natural units, i.e. $\hbar = 1$, $c = 1$.

1.3.1 Our study

For the energy shift caused by a one-loop VP we have

$$\Delta E_{\rm VP} = \langle \psi_{\rm at} | V_{\rm VP} | \psi_{\rm at} \rangle, \tag{1.27}$$

where the potential $V_{\rm VP}$ is generated by the vacuum charge density $\langle \rho(\mathbf{r}) \rangle$ which is given by the expression

$$\langle \rho(\mathbf{r}) \rangle = -ie \int_C \frac{{\rm d}E}{2\pi} \langle \mathbf{r} | {\rm Tr} \gamma_0 \frac{1}{\gamma \cdot \Pi - m_{\rm loop}} | \mathbf{r} \rangle. \tag{1.28}$$

where $\mathbf{r}$ is the position vector, C is a countour over which we integrate, Π is the four-momentum of the electron in an external Coulomb field $\Pi = \left(E + \frac{Z\alpha}{r}, \mathbf{p}\right)$

and γ_μ are the Dirac matrices. Derivation of this formula from the basic principles and description of the countour can be found in [35], Sec. 2.2.

In this section we give a simplified but transparent description of our method which is in detail presented in [35]. In short, it consists of three steps:

1. We reduce the problem to a calculation of Laplace transform of the vacuum charge density $\langle\rho(\mathbf{r})\rangle$ (1.28).

2. We use the spectral decomposition of the Dirac Hamiltonian and the two formulae for hypergeometric functions.

3. After charge renormalization we express the Laplace transform of the $V_{\rm VP}$ in the order of $\alpha(Z\alpha)^4$ (Uehling potential [29]) and $\alpha(Z\alpha)^6$ (Wichmann-Kroll potential [30]) and calculate the caused energy shifts.

1.3.2 Reduction to Laplace transform

The energy shift of the ground state of the hydrogen-like atom caused by vacuum polarization reads

$$\Delta E = \int \mathrm{d}^3\mathbf{r}|\psi_0(\mathbf{r})|^2 V_{\rm VP}(\mathbf{r}) = N_0^2 \int \mathrm{d}^3\mathbf{r}\exp\{-\beta r\}V_{\rm VP}(\mathbf{r})\,, \tag{1.29}$$

where we substituted for the probability density

$$|\psi_0(\mathbf{r})|^2 = N_0^2\exp\{-\beta r\}, \quad N_0^2 = \frac{(m_r Z\alpha)^3}{\pi}, \quad \beta = 2m_r Z\alpha\,. \tag{1.30}$$

The energy shift of the excited states can be obtained by differentitation with respect to parameter β, for details see Sec. 1.3.5.

The potential created by vacuum charge density $\langle\rho(\mathbf{r})\rangle$ satisfies Poisson equation

$$-\nabla^2 V_{\rm VP}(\mathbf{r}) = e\langle\rho(\mathbf{r})\rangle\,. \tag{1.31}$$

Following [30] we take Laplace transform of this equation. That is, we multiply this equation by $\exp\{-\beta r\}$ and integrate over the whole space. The parameter β, later transformed to dimensionless parameter b, is used as a Laplace transformed function variable. The Laplace transform of the Poisson equation (1.31) leads to the relation

$$\frac{d}{d\beta}\left[\beta^2 U(\beta)\right] = q(\beta) \;\Rightarrow\; U(\beta) = \beta^{-2}\int_0^\beta \mathrm{d}\beta' q(\beta'), \tag{1.32}$$

where function $q(\beta)$ is the Laplace tranform of the vacuum charge denstity defined as

$$q(\beta) = \int \mathrm{d}^3\mathbf{r}\exp\{-\beta r\}e\langle\rho(\mathbf{r})\rangle\,; \tag{1.33}$$

and function $U(\beta)$ is the Laplace tranform of the VP potential defined as

$$U(\beta) = \int \frac{\mathrm{d}^3\mathbf{r}}{r}\exp\{-\beta r\}V_{\rm VP}(\mathbf{r})\,. \tag{1.34}$$

The details of the derivation of the relation (1.32) can be found in [35], Sec. 2.2.

Since the energy shift (1.29) can be easily expressed through the function $U(\beta)$, we obtain the sought relation between energy shift and the Laplace transform of the charge density

$$\Delta E = N_0^2\left(-\frac{\mathrm{d}}{\mathrm{d}\beta}\right)U(\beta) = N_0^2\left(-\frac{\mathrm{d}}{\mathrm{d}\beta}\right)\left[\beta^{-2}\int_0^\beta \mathrm{d}\beta' q(\beta')\right]. \tag{1.35}$$

1.3.3 Calculation of Laplace transform charge density

In this section we describe the calculation of the function $q(\beta)$, which is needed to get the energy shift from the relation (1.35). This consists of several important steps. First, we rewrite the definition of $\langle\rho(\mathbf{r})\rangle$ in Eq. (1.28),

$$\langle\rho(\mathbf{r})\rangle = -ie\int\frac{\mathrm{d}E}{2\pi}\langle\mathbf{r}|\gamma_0\frac{(\gamma\cdot\Pi+m_{\mathrm{loop}})}{(\gamma\cdot\Pi+m_{\mathrm{loop}})(\gamma\cdot\Pi-m_{\mathrm{loop}})}|\mathbf{r}\rangle = \\ = e\int_C\frac{\mathrm{d}E}{2\pi i}\langle\mathbf{r}|\mathrm{Tr}(E+\frac{Z\alpha}{r}-\gamma_0\gamma\cdot\hat{\mathbf{p}}+\gamma_0 m_{\mathrm{loop}})\frac{1}{\mathcal{H}}|\mathbf{r}\rangle, \quad (1.36)$$

In the last equation we have introduced the so called second order Dirac Hamiltonian [5], which, in our case has the form

$$\hat{\mathcal{H}} = E^2 - m_{\mathrm{loop}}^2 + 2\frac{EZ\alpha}{\hat{r}} - \left(\hat{p}_r^2 + \frac{l(l+1)}{\hat{r}^2}\right), \quad (1.37)$$

where $\hat{p}_r$ is a radial momentum operator and l is an effective orbital number defined as

$$l = \begin{cases}\sqrt{\left(j+\frac{1}{2}\right)^2-(Z\alpha)^2}-1\,,\\ \sqrt{\left(j+\frac{1}{2}\right)^2-(Z\alpha)^2}\,.\end{cases} \quad (1.38)$$

We choose value of l from the two cases in Eq. (1.38) depending on the eigenvalue of other operator, for more see Sec. 2.3 of [35]. We rewrite the expression (1.36) in this way because $\hat{\mathcal{H}}$ is structurally identical to Schrödinger Hamiltonian and has higher symmetry than the first order Hamiltonian, the denominator in expression (1.28). This allows us to use a spectral decomposition in eigenfunctions of $\hat{\mathcal{H}}$. Spinor-angular part of these eigenfuctions consists of well-known spherical spinors and the radial part of eigenfunctions of this operator belonging to the continuous part of the spectrum are [17]

$$R_l(p,r) = \sqrt{\frac{2}{\pi}}\frac{p\mathrm{e}^{\frac{\pi EZ\alpha}{2p}}|\Gamma(l+1-iEZ\alpha/p)|}{\Gamma(2l+2)}\times \\ \times(2pr)^l\mathrm{e}^{-ipr}F\left(\frac{iEZ\alpha}{p}+l+1,\,2l+2,\,2ipr\right), \quad (1.39)$$

where $F(\alpha,\gamma,z)$ is the confluent hypergeometric function [17]. The eigenfunctions belonging to the discrete part of the spectrum are inessential for our purpose.

In the next step we utilize the spectral decomposition of the second order Dirac Hamiltonian $\hat{\mathcal{H}}$ (1.37) and we integrate over spinor-angular degrees of freedom. Althoug technical and lengthy, it is rather a straightforward procedure described in Sec. 2.4 of [35]. We get the function $q(\beta)$ in the form

$$q(\beta) = 8\alpha\sum_{k=1}^{\infty}k\int_C\frac{\mathrm{d}E}{2\pi i}\int_0^\infty\frac{\mathrm{d}p}{E^2-p^2-m_{\mathrm{loop}}^2}\times \\ \times\left\{E\left(-\frac{\partial}{\partial\beta}\right)+Z\alpha\left(1+\frac{\beta}{2\Gamma}\frac{\partial}{\partial\beta}\right)\right\}I_l(p,\beta)\,, \quad (1.40)$$

where $k = j + 1/2$ and

$$I_l(p,\beta) = 2\pi \int_0^\infty \mathrm{d}r\, r\mathrm{e}^{-\beta r} |R_l(p,r)|^2 \,. \tag{1.41}$$

The complicated part is finding the integral (1.41) in a form that can be integrated over E in the next step. To evaluate the integral, we use two formulae for hypergeometric functions. The first formula reads [17]:

$$\int_0^\infty \mathrm{d}r \exp\{-\lambda r\} r^{\gamma-1} F(\alpha,\gamma,kr) F(\alpha',\gamma,k'r) = \Gamma(\gamma)\lambda^{\alpha+\alpha'-\gamma} \times$$
$$\times (\lambda-k)^{-\alpha}(\lambda-k')^{-\alpha'} F(\alpha,\alpha',\gamma,z), \quad z = \frac{kk'}{(\lambda-k)(\lambda-k')} \,. \tag{1.42}$$

The second formula reads [10]:

$$F(\alpha,\alpha',\gamma,z) = \frac{\Gamma(\gamma)}{\Gamma(\alpha')\Gamma(\gamma-\alpha')} \int_0^1 \mathrm{d}t\, \frac{t^{\alpha'-1}(1-t)^{\gamma-\alpha'-1}}{(1-tz)^\alpha},$$
$$\mathrm{Re}(\gamma) > \mathrm{Re}(\alpha') > 0, \quad \arg(1-z) < \pi. \tag{1.43}$$

Using these two formulae and further manipulation, we find the integral $I_l(p,\beta)$ and after integration over E also a convenient expression for $q\,(\beta)$. For details see Sec. 2.5 of [35].

1.3.4 Summation over partial waves, expansion in $Z\alpha$ and renormalization

Further, we have the sum over partial waves. It can be done either numerically or analytically with an approximation. The former approach is used for example in [28] and is useful for cases with high Z. We use expansion of the effective orbital number l (1.38) and the hyperbolic functions in $Z\alpha$. This allows us to carry out the summation over k from 0 to ∞ in Eq. (1.40) analytically. The detailed description of the manipulations and simplifications can be found in Secs. 2.6-8 of [35].

The integrals in (1.40) are divergent in p and we renormalize them in the Pauli-Villars manner by subtracting from the non-renormalized expression the contribution of another pair of heavy fermions with mass[8] M. The procedure is not trivial and we explain it in detail in Sec. 3 of [35].

We then express the result in terms of a dimensionless parameter b that is related to the parameter β as follows

$$b = \frac{\beta}{2m_{\mathrm{loop}}} = \frac{m_r}{m_{\mathrm{loop}}} Z\alpha \,. \tag{1.44}$$

Up to order $\alpha\,(Z\alpha)^3$ it holds for the renormalized Laplace transform of the charge density $\overline{q}(b)$

$$\overline{q}(b) \simeq -4\alpha(Z\alpha)\frac{\mathrm{d}}{\mathrm{d}b}\overline{Q}(b), \quad \overline{Q}(b) = \overline{Q}_1(b) + (Z\alpha)^2\overline{Q}_3(b), \tag{1.45}$$

[8] It is given in units of m_{loop}^2.

where

$$\overline{Q}_1(b) = \int_0^\infty \mathrm{d}p \left\{ \left[\sqrt{1+(bp)^2} - 1 - \frac{(bp)^2}{2} \right] \left[1 - p \arctan\left(\frac{1}{p}\right) - \frac{1}{3p^2} \right] - \right.$$
$$\left. - \frac{1}{2} \left[\frac{1}{\sqrt{1+(bp)^2}} - 1 + \frac{(bp)^2}{2} \right] \frac{\ln(1+p^2) - 2\ln(p)}{p^2} \right\} \quad (1.46)$$

and

$$\overline{Q}_3(b) = \int_0^\infty \mathrm{d}p \left\{ -\frac{1}{2} \left[\sqrt{1+(bp)^2} - 1 - \frac{(bp)^2}{2} \right] \frac{1 - p\arctan\left(\frac{1}{p}\right)}{p^2} \times \right. \quad (1.47)$$
$$\times \int_0^1 \frac{\mathrm{d}t}{t(1-t)} \frac{s(1+s)\ln(s)}{1-s} + \left[\frac{[1+(bp)^2]^{3/2}}{b^2} - \frac{1}{b^2} - \frac{3}{2}p^2 - \frac{3}{8}b^2p^4 \right] \times$$
$$\times \left[- \frac{\left[2\arctan\left(\frac{1}{p}\right)\right]^3 - 2\arctan\left(\frac{1}{p}\right)\left[\pi^2 - 6\,\mathrm{dilog}\left(\frac{1}{p^2+1}\right)\right]}{12p} - \frac{\frac{1}{3} + 2\ln(p)}{p^4} \right] +$$
$$+ \left[\sqrt{1+(bp)^2} - 1 - \frac{(bp)^2}{2} - \mathrm{arctanh}\left(\frac{1}{\sqrt{1+(bp)^2}}\right) - \ln\left(\frac{pb}{2}\right) + \frac{(pb)^2}{4} \right] \times$$
$$\times \left[\frac{\left[2\arctan\left(\frac{1}{p}\right)\right]^2}{2} - \frac{\pi^2 - 6\,\mathrm{dilog}\left(\frac{1}{p^2+1}\right)}{6} - \frac{1 - 2\ln(p)}{p^2} \right] +$$
$$+ \left[\frac{1}{\sqrt{1+(bp)^2}} - 1 + \frac{(bp)^2}{2} \right] \times$$
$$\times \left[- \frac{\int_0^1 \frac{\mathrm{d}t}{t(1-t)}(1-s)\left[\ln(1-s)\ln(s) + \mathrm{dilog}(1-s)\right]}{4p^2} + \frac{\zeta(3)}{p^2} \right] +$$
$$+ \left[\mathrm{arctanh}\left(\frac{1}{\sqrt{1+(bp)^2}}\right) + \ln\left(\frac{pb}{2}\right) - \frac{(pb)^2}{4} \right] \times$$
$$\left. \times \left[\frac{\left[2\arctan\left(\frac{1}{p}\right)\right]^2 \ln(1+p^2) - \int_0^1 \frac{\mathrm{d}t}{t(1-t)} s \ln^2\left(\frac{1-t}{t[1-tz(p)]}\right)}{4p^2} + \frac{\zeta(3)}{p^2} \right] \right\}.$$

Usually, the $\overline{Q}_1(b)$ is called Uehling term [29] and $\overline{Q}_3(b)$ is called Wichmann-Kroll term [30].

The energy shift (1.35) can be also expressed in terms of dimensionless variable b and renormalized functions $\overline{q}(b)$ or $\overline{Q}(b)$ connected by relation (1.45) as

$$\Delta E = m_{\mathrm{loop}} \left(\frac{m_r}{m_{\mathrm{loop}}}\right)^2 \frac{(Z\alpha)^3}{4\pi} \left(-\frac{\mathrm{d}}{\mathrm{d}b}\right) \left[b^{-2} \int_0^b \mathrm{d}b' \overline{q}(b') \right] \Big|_{b=\frac{m_r}{m_{\mathrm{loop}}}Z\alpha} =$$
$$= m_{\mathrm{loop}} \left(\frac{m_r}{m_{\mathrm{loop}}}\right)^2 \frac{\alpha(Z\alpha)^4}{\pi} \frac{\mathrm{d}}{\mathrm{d}b} \left[b^{-2} \overline{Q}(b) \right] \Big|_{b=\frac{m_r}{m_{\mathrm{loop}}}Z\alpha}. \quad (1.48)$$

1.3.5 Results

At this point we give the numerical results obtained from formulae (1.46) and (1.47) for electronic VP, therefore we take $m_{\mathrm{loop}} = m_e$. In the case of ordinary hydrogen for which $b << 1$ we can further expand the expressions in b

$$\overline{Q}_1(b) = \overline{Q}_{13} b^3 + \overline{Q}_{14} \frac{b^4}{2} + \dots\,, \qquad \overline{Q}_3(b) = \overline{Q}_{33} b^3 + \overline{Q}_{34} \frac{b^4}{2} + \dots\,. \tag{1.49}$$

For the coefficients in (1.49) taken from expansions of (1.46) and (1.47) we get

$$\overline{Q}_{13} = -\frac{4}{15}\,, \tag{1.50}$$

$$\overline{Q}_{14} = \frac{5\pi}{48}\,, \tag{1.51}$$

$$\overline{Q}_{33} = \frac{19}{45} - \frac{\pi^2}{27}\,, \tag{1.52}$$

$$\overline{Q}_{34} = \left(\frac{1}{16} - \frac{31\pi^2}{2880}\right)\pi\,. \tag{1.53}$$

These results are in an agreement with those found in [30]. We have obtained the last result only numerically; we have reproduced it to nine digits.

The case of muon hydrogen is more complicated because $b \simeq 1.36$; therefore, the expansion (1.49) is inapplicable. We have to evaluate the terms (1.46) and (1.47) without any further approximation, hence we integrate over p and t numerically. We omit the integration of $\overline{Q}_1(b)$ which is well known and we concetrate on $\overline{Q}_3(b)$. For the energy shift of the ground state (1.48) caused by the Wichmann-Kroll term (1.47) we have

$$(\Delta E)_{\mathrm{WK}}\,(1\mathrm{s}) = m_e \left(\frac{m_r}{m_e}\right)^3 \frac{\alpha(Z\alpha)^6}{\pi}\,\frac{\mathrm{d}}{\mathrm{d}b}\left[b^{-2}\overline{Q}_3(b)\right]\Big|_{b=\frac{m_r}{m_e}Z\alpha}\,, \quad m_r = \frac{m_\mu}{1+\frac{m_\mu}{m_p}}\,. \tag{1.54}$$

We are mostly interested in the contribution of the Wichmann-Kroll term to the Lamb shift, hence we need the formula for the energy shifts of 2p and 2s states. For non-S-states it is thus sufficient to consider the angular average of the probability density of the reference state, because the induced charge density is spherically symmetric. For the probability density of the excited states we have

$$|\psi_{2\mathrm{s}}(r)|^2 = \frac{N_0^2}{8}\mathrm{e}^{-\beta r}\left(1 - \beta r + \frac{\beta^2 r^2}{4}\right)$$

and

$$\int \frac{\mathrm{d}\,\Omega}{4\pi}|\psi_{2\mathrm{p}}(\mathbf{r})|^2 = \frac{N_0^2}{96}\mathrm{e}^{-\beta r}\beta^2 r^2$$

where β, N_0 and b are given by

$$\beta = m_r Z\alpha\,, \qquad N_0^2 = \frac{(m_r Z\alpha)^3}{\pi}\,, \qquad b = \frac{m_r}{2m_e}Z\alpha\,.$$

The energy shift for these states is obtained by the method of differentiation of an integral with respect to a parameter[9].

$$(\Delta E)_{\mathrm{WK}}(2\mathrm{s}) = m_e \left(\frac{m_r}{m_e}\right)^3 \frac{\alpha(Z\alpha)^6}{\pi}\frac{1}{8}\times \\ \times \left(1 + b\frac{\mathrm{d}}{\mathrm{d}b} + \frac{b^2}{4}\frac{\mathrm{d}^2}{\mathrm{d}b^2}\right)\frac{\mathrm{d}}{\mathrm{d}b}\left[b^{-2}\overline{Q}_3(b)\right]\Big|_{b=\frac{m_r}{2m_e}Z\alpha} \tag{1.55}$$

and

$$(\Delta E)_{\mathrm{WK}}(2\mathrm{p}) = m_e \left(\frac{m_r}{m_e}\right)^3 \frac{\alpha(Z\alpha)^6}{\pi}\frac{1}{96}b^2\frac{\mathrm{d}^2}{\mathrm{d}b^2}\,\frac{\mathrm{d}}{\mathrm{d}b}\left[b^{-2}\overline{Q}_3(b)\right]\Big|_{b=\frac{m_r}{2m_e}Z\alpha}. \tag{1.56}$$

We can now plug in the numerical values of the used constants [18]

$$\alpha = \frac{1}{137.035999074}, \tag{1.57}$$

$$\frac{m_e}{m_\mu} = 4.83633166\,10^{-3}, \tag{1.58}$$

$$\frac{m_e}{m_p} = 5.4461702178\,10^{-4}, \tag{1.59}$$

$$m_e = 0.510998928\,10^6\,\mathrm{eV}, \tag{1.60}$$

and then we perform the numerical calculations. Unfortunately, the integration is not stable for $p \to 0$ and $p \to \infty$. We thus split the integration over p from 0 to infinity into three regions. Region I is for $p \in (0, 0.2)$, region II for $p \in (0.2, 30)$ and region III for $p \in (30, \infty)$. We first expand (1.47) into the series in p and then integrate in the region I term by term over t and p until the result is stable[10]. In region II we perform the complete two-dimensional numerical integration. This is the dominant part of the effect. In region III we use the asymptotic expansion of $\overline{Q}_3(b)$ valid for large p and again integrate term by term.

For the contribution of the Wichmann-Kroll term to the Lamb shift in muonic hydrogen we obtain

$$(\Delta E)_{\mathrm{WK}}(2\mathrm{p}) - (\Delta E)_{\mathrm{WK}}(2\mathrm{s}) \simeq -0.10158\,10^{-5}\mathrm{eV} \tag{1.61}$$

which differs by 1% from the result $-0.103\,10^{-5}$eV given in [15].

1.3.6 Discussion

The difference between our result and that given in [15] is not surprising. The calculation here is for what is to be the exact form of WK pontential, while the result obtained in [7, 15] is obtained using an approximate form of the WK potential. The approximate formula fits the exact potential with an accuracy of about 1% [9].

On the other hand, we have used in our treatment a nonrelativistic wave function of the reference state. The error of this approximation is negligible at the present level of accuracy because the difference between the nonrelativistic and relativistic treatment of the reference wave function is of the order $\alpha(Z\alpha)^8$, probably multiplied by $\ln(Z\alpha)$.

[9] We use the following feature of the Laplace transform: $\mathcal{L}[rf(r)](p) = -\frac{\mathrm{d}}{\mathrm{d}p}\mathcal{L}[f(r)](p)$.

[10] It does not change on relevant digits when adding more terms

1.4 Self-energy Vacuum polarization correction

The dominant effect to the Lamb shift is due to the electronic one-loop VP. Thus, it is reasonable to assume that the combined self-energy vacuum polarization corrections are significant. The Feynman diagrams of these corrections are shown in Fig. 1.6.

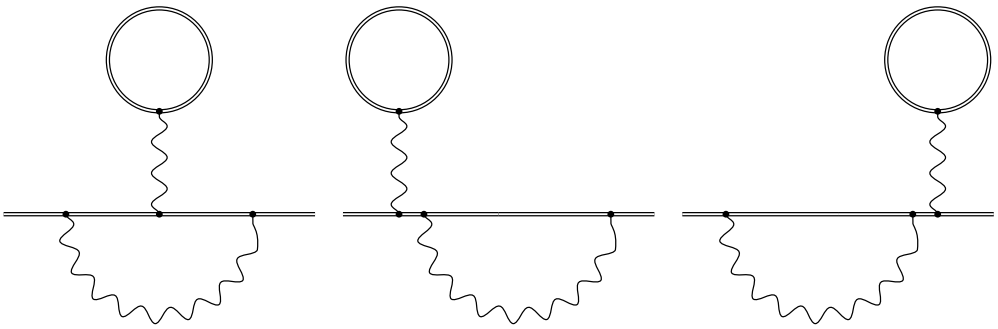

Figure 1.6: Electronic self-energy vacuum polarization effect

Here we calculate this effect in the lowest order, i.e. we combine leading orders of SE and VP, specifically the leading order of relativistic multipole expansion (RME) [32, 33] with the Uehling potential.

1.4.1 Energy shift

The leading order of RME yields the self-energy effect of the bound particle with mass m in the form [32]

$$\Delta E_{\mathrm{SE}} = m\frac{\alpha}{\pi N^3}(Z\alpha)^4\left(\frac{m_r}{m}\right)^3 F(Z\alpha)\,, \quad F = F_{\mathrm{low}} + F_{\mathrm{high}}, \tag{1.62}$$

where N is the principal quantum number of the reference state ψ_{at}. The consequence of the use of RME is that the dimensionless function F is divided into two parts. The low-energy term, called here the extended Bethe logarithm (EBL), has the form

$$F_{\mathrm{low}} = \langle\psi_{\mathrm{at}}|p_i f\,(h-e_N)\,p_i|\psi_{\mathrm{at}}\rangle\,,$$
$$f(x) = N^3 x\int_0^1 \mathrm{d}y\int_0^1 \mathrm{d}w\frac{1-2w(1-w)}{y+w2(Z\alpha)^2\frac{m_r}{m}x}\,, \tag{1.63}$$

where p_i is the momentum, $h = p^2/2+v(r)$ is the nonrelativistic Hamiltonian operator, $v(r)$ is the potential[11] and $e_N = -1/(2N^2)$ is the nonrelativistic energy of the reference state. All these quantities are given in atomic units. The expansion of the function $f(x)$ yields

$$f(x) = N^3 x\left(\frac{13}{8} - \frac{2}{3}\ln[2(Z\alpha)^2\frac{m_r}{m}x] + \ldots\right). \tag{1.64}$$

If we insert this expansion back into (1.63), the first term of the form

$$\frac{N^3}{2}\langle\psi|p_i(h-e_N)\ln(h-e_N)p_i|\psi\rangle \tag{1.65}$$

[11] In the case of Coulomb potential, $v(r) = -1/r$.

is usually called Bethe logarithm [4]. The high-energy part of the effect is

$$F_{\rm high} = N^3 \langle\psi_{\rm at}| \left\{ -\frac{1}{12}\nabla^2 v(r) + \frac{1}{2}\frac{\hat{\mathbf{S}}\cdot\hat{\mathbf{L}}}{r}\left[\frac{\rm d}{{\rm d}r}, v(r)\right] + \frac{m}{2M}\frac{\hat{\mathbf{S}}\cdot\hat{\mathbf{L}}}{r^3}\right\} |\psi_{\rm at}\rangle \,, \quad (1.66)$$

where $\hat{\mathbf{S}}$ is the spin operator and $\hat{\mathbf{L}}$ is the orbital momentum operator. Here we include the coupling between the spin of the electron and the nucleus orbit due to the anomalous magnetic moment of the electron, i.e. a part of the radiative-recoil contribution. The detailed description of the effect can be found in [20], Sec. III.

1.4.2 Calculation

We are interested in the combined SE and electron VP effect, specifically the part of the effect where the Uehling potential modifies the electron propagator and the wave function of the reference state, cf. Fig. 1.6. We now modify the Coulomb potential and add the Uehling potential V_U, which is given by (1.31), where we take the vacuum charge density in the first order (1.46). After transformation to the coordinate space [29] and transition to atomic units we get

$$-\frac{1}{r} \to -\frac{1}{r} + v_U, \quad v_U = \int_0^1 {\rm d}x\, U(x) \frac{e^{-\mu(x) r}}{r} \,, \quad (1.67)$$

where $U(x) = \frac{x\left(1-\frac{2}{3}x\right)(1-2x)}{1-x}$ and $\mu(x) = \frac{m_e}{m_r(Z\alpha)}\frac{1}{\sqrt{x(1-x)}}$. We treat v_U as the perturbation to the Coulomb potential and we calculate the function F in Eq. (1.62) to the first order. To do that we employ the method of pseudostates, the expansion of the exact wave functions into entirely discrete basis sets. The description of this method is given in [20], Sec. IV. The first perturbation to the low-energy part is given by the sum

$$F^1_{\rm low} = (F^1_{\rm low})_{\rm wf} + (F^1_{\rm low})_{\rm ver} + (F^1_{\rm low})_{\rm en} \,, \quad (1.68)$$

where

$$(F^1_{\rm low})_{\rm wf} = -2 \sum_{m=L+1\neq N}^{L+M} \sum_{q=l+1}^{l+Q} \int_0^1 {\rm d}x\, U(x) \langle\psi^0_{N,L}| \frac{{\rm e}^{-\mu(x) r}}{r} |\psi^0_{m,L}\rangle \times$$
$$\times \langle\psi^0_{m,L}|p_i|\psi^0_{q,l}\rangle\langle\psi^0_{q,l}|p_i|\psi^0_{N,L}\rangle \frac{f(e^0_q - e^0_N)}{e^0_m - e^0_N} \quad (1.69)$$

comes from the correction to the wave function of the reference state,

$$(F^1_{\rm low})_{\rm ver} = \sum_{q=l+1}^{l+Q} \left\{ \sum_{m=l+1\neq n}^{l+Q} \langle\psi^0_{N,L}|p_i|\psi^0_{m,l}\rangle \int_0^1 {\rm d}x\, U(x) \langle\psi^0_{m,l}| \frac{{\rm e}^{-\mu(x) r}}{r} |\psi^0_{q,l}\rangle \times \right.$$
$$\times \langle\psi^0_{q,l}|p_i|\psi^0_{N,L}\rangle \frac{f(e^0_m - e^0_N) - f(e^0_q - e^0_N)}{e^0_m - e^0_q} +$$
$$\left. + \langle\psi^0_{N,L}|p_i|\psi^0_{q,l}\rangle \int_0^1 {\rm d}x\, U(x) \langle\psi^0_{q,l}| \frac{{\rm e}^{-\mu(x) r}}{r} |\psi^0_{q,l}\rangle \langle\psi^0_{q,l}|p_i|\psi^0_{N,L}\rangle \frac{{\rm d}f(e^0_q - e^0_N)}{{\rm d}e^0_q} \right\} \quad (1.70)$$

is the vertex correction and

$$(F^1_{\rm low})_{\rm en} = \sum_{q=l+1}^{l+Q} \langle\psi^0_{N,L}|p_i|\psi^0_{q,l}\rangle\langle\psi^0_{q,l}|p_i|\psi^0_{N,L}\rangle\times \\ \times\int_0^1 {\rm d}x\, U(x)\langle\psi^0_{N,L}|\frac{{\rm e}^{-\mu(x)r}}{r}|\psi^0_{N,L}\rangle\frac{{\rm d}f(e^0_q-e^0_N)}{{\rm d}e^0_q} \quad (1.71)$$

comes from the correction to the energy of the reference state. Function $|\psi^0_{N,L}\rangle$ is the reference function, $|\psi^0_{m,l}\rangle$ and $|\psi^0_{q,l}\rangle$ are called Sturmian functions which form a complete basis set.

Further, we consider high energy part (1.66) of the effect. The first order perturbation due to the Uehling potential is a sum of two contributions

$$F^1_{\rm high} = (F^1_{\rm high})_{\rm wf} + (F^1_{\rm high})_{\rm pot}, \quad (1.72)$$

where the former is due to the correction to the wave function

$$(F^1_{\rm high})_{\rm wf} = -2\sum_{m=L+1\neq N}^{L+M}\langle\psi^0_{N,L}|\left[-\frac{\pi}{3}\delta^3(\mathbf{r})+\frac{m_\mu+M}{2M}\frac{\mathbf{S}\cdot\mathbf{L}}{r^3}\right]|\psi^0_{m,L}\rangle\times \\ \times\int_0^1 {\rm d}x\, U(x)\langle\psi^0_{m,L}|\frac{e^{-\mu(x)r}}{r}|\psi^0_{N,L}\rangle\frac{1}{e^0_m-e^0_N}\,, \quad (1.73)$$

and the latter is caused by the modification of the Coulomb potential by the Uehling potential

$$(F^1_{\rm high})_{\rm pot} = \int_0^1 {\rm d}x\, U(x)\langle\psi^0_{N,L}|e^{-\mu(x)r}\times \\ \times\left[\frac{\pi}{3}\delta^3(\mathbf{r})-\frac{\mu(x)^2}{12r}-\frac{1}{2}\frac{\mathbf{S}\cdot\mathbf{L}}{r^3}(1+\mu(x)r)\right]|\psi^0_{N,L}\rangle. \quad (1.74)$$

The detailed derivations of the the matrix-elements formulae of the type

$$\langle\psi^0_{m,l}|g|\psi^0_{q,l}\rangle\,, \qquad g\in\left\{p_i,\,\delta^3(\mathbf{r}),\,\frac{1}{r},\,\frac{{\rm e}^{-\mu r}}{r},\,\frac{1}{r^3}\right\}, \quad (1.75)$$

are either trivial or given in Sec. IV.E and Apendices B, C, D of [20]. Summations over q and/or m in Eqs. (1.68), (1.70), (1.71) and (1.73) are in principle infinite. We calculate it for different values of the upper limit and extrapolate the result. All integrations over r can be done analytically, over parameter x we have to integrate numerically.

1.4.3 Results and discussion

The results for both low- and high-energy parts from equations (1.68) and (1.72) for states $1s-4s$ and $2p-4p$ are given in Tab. 1.2. The evaluation is more difficult for S-states. We thus obtain for the contribution of the SEVP effect considered here to the Lamb shift in muonic hydrogen an energy shift

$$\Delta E(2{\rm p}_{\frac{1}{2}}) - \Delta E(2{\rm s}) \simeq -2.706\times10^{-6}\,{\rm eV},$$

which differs by 8% from the result $-2.5\times10^{-6}\,{\rm eV}$ given in [13]. Some difference can be expected because our method is more accurate, i.e. it includes a larger portion of the SEVP effect in comparison with the calculation involving ordinary Bethe logarithm (1.65).

State	F^1_{low}	F^1_{high}	F^1
1s	20.330	-0.871	19.459
2s	18.900	-0.772	18.129
3s	18.33	-0.745	17.585
4s	18.02	-0.731	17.289
$2p_{\frac{1}{2}}$	-0.274	-0.039	-0.313
$2p_{\frac{3}{2}}$		0.028	-0.246
$3p_{\frac{1}{2}}$	-0.286	-0.043	-0.329
$3p_{\frac{3}{2}}$		0.031	-0.255
$4p_{\frac{1}{2}}$	-0.288	-0.044	-0.332
$4p_{\frac{3}{2}}$		0.032	-0.256

Table 1.2: Magnitudes of F^1_{low} and F^1_{high} for the muonic hydrogen where the Coulomb potential is perturbed by the Uehling potential. Further, $F^1 = F^1_{\text{low}} + F^1_{\text{high}}$.

2. Multi-Dimensional Tunneling

2.1 Motivation

Tunneling is a name used for a quantum phenomenon where a particle gets across a barrier that could not overcome classically. The tunneling is well understood in cases of one-dimensional or separable multi-dimensional potentials, for exhaustive review see [57]. On the other hand, tunneling in non-separable multi-dimensional potentials still poses a challenge [36, 39].

Tunneling has been studied in a wide variety of fields, among others the theory of chemical reactions [36], false vacuum states in quantum field theory [38], nuclear fusion or fission [44], scanning tunneling spectroscopy [43] and others, for more references see for example this review [47].

Nowadays, it is possible to describe sufficiently small molecules using time-independent quantum-chemical methods and get theoretical results that are in good agreement with molecular spectroscopy measurements. This is not the case for molecules like malonaldehyde with resonance structures displayed in Fig. 2.1.

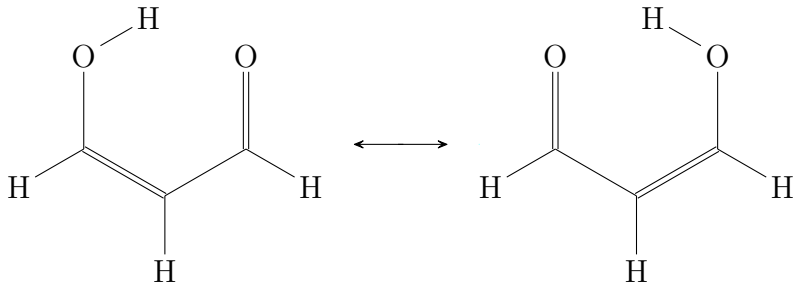

Figure 2.1: Two contributing structures of malonaldehyde

The proton (bound to one of the oxygens) tunnels through a potential barrier and gives rise to a doublet which can be detected by means of microwave spectroscopy [40].

In the following sections we first give an overview of the attempts to describe tunneling, then we present our method and discuss the results.

2.2 Brief review of methods describing the tunneling

The approaches used to calculate energy splittings due to tunneling can be sorted into two cathegories. One can either try to directly solve a Schrödinger equation or use an approximative scheme.

The former approach is more accurate, but it is only applicable to small systems because these methods are computationally demanding. One of such methods is multiconfigurational time-dependent Hartree-Fock calculations [42], where large enough basis has to be used. Other methods employ formalism of path integrals [45, 51]. Although still formally exact, it is burdened by the

statistical error which needs to be reduced by sampling over many configurations, thus again, using much computer time.

The latter approach make an approximation to Schrödinger equation and solve the problem without sampling or expansion in finite basis. Since the standard Rayleigh-Schrödinger perturbation (RSP) method does not usually work[1], the semi-classical (also called WKB) approach [36, 46] is used. Its usual disadvantage is that it requires prior knowledge of the tunneling path [36][2]. Closely related to WKB is an instanton[3] approach [46, 47, 49], although derived as an approximation from path integral formalism[4].

The WKB expansion and instanton method require specific trajectories, i.e. tunneling path and instanton, resp. The method suggested by Milnikov *et al.* in [46], described in detail in [47], is applicable to real polyatomic systems in the full dimensionality. Other practical method [49] was inspired by this. The method of Milnikov *et al.* also includes variational procedure for finding the instanton and a scheme to incorporate *ab initio* data. The method might seem to be the solution of the problem, but there are several resons why it should not suffice. First of all, it is exact only up to the zeroth order in $\hbar$. Even more, we show that for some potentials, including the case of malonaldehyde, this approximation is not valid. It can be seen even from the results in [47], where authors get the energy splitting in malonaldehyde between 4.5 to 77 cm^{-1} when different *ab initio* methods/basis are taken. Other works usually estimate the splitting within a factor of 2 compared to the experimental result 21.6 cm^{-1} [40]. Further, it is a numerical method; thus, it does not provide global insight.

Other methods are based on reduced dimensionality [52], i.e. constructing an effective one-dimensional potential and use an existing one-dimensional method that generally works well. Here we show that in this approach many important features of the problem are lost.

2.3 Our study

In this section we give a description of a method and results given in the article [56] which is based on a method introduced in [54]. After more thorough introduction to the problem, we discuss here variational calculations and application of RSP method.These are well known and omitted in the article [56], but the reader can benefit from a summarization and explanation of those methods in our specific case. We then introduce our method with emphasis on the key ideas. We skip here some technical details like the description of the numerical analysis of the series or some transformations between functions we get in the intermediate steps. A comprehensive description is given in the article [56].

[1] This will be discussed more in Sec. 2.3.6

[2] In this work we use a different WKB expansion [54] that does not require knowledge of the tunneling path.

[3] The dominant imaginary-time tunneling path.

[4] The connection is described eg. in [46].

2.3.1 Definition of the problem

We are interested in the calculation of a ground-state tunneling splitting in a two-dimensional double-well potential with the reflection symmetry. Potentials of this class are important for understanding of spectroscopy of non-rigid molecules such as malonaldehyde in Fig. 2.1.

We take the potential in the form

$$V(x,y) = \frac{(x^2-R^2)^2}{8R^2} + \frac{x^2-R^2}{R^2}\gamma y + \frac{\omega^2}{2}y^2\,. \tag{2.1}$$

This type of potential has been previously used in works [36, 37], although in a different form.

The potential $V(x,y)$ is characterized by three parameters (R,ω,γ) which successively describe:

1. R – the height and thickness of the barrier between the wells, the reciprocal value is equivalent to the Planck constant $1/R \sim \hbar$,

2. ω – the steepness of the potential in y relatively to x,

3. γ – the coupling between oscilations in x and y direction.

We assume $\gamma < \gamma_s = \omega R/2$, which means there are two wells located at $(x,y) = (\pm R, 0)$ and a saddle-point at $(x,y) = (0, \gamma/\omega^2)$. If $\gamma > \gamma_s$, the potential would have two saddle-points at $(x,y) = (\pm R, 0)$ and a well at $(x,y) = (0, \gamma/\omega^2)$ and it would no longer be a model system for tunneling. The potential is symmetric with respect to the reflection around y-axis, $V(x,y) = V(-x,y)$. The countour plot of the potential for physically relevant parameters can be seen in Fig. 2.2.

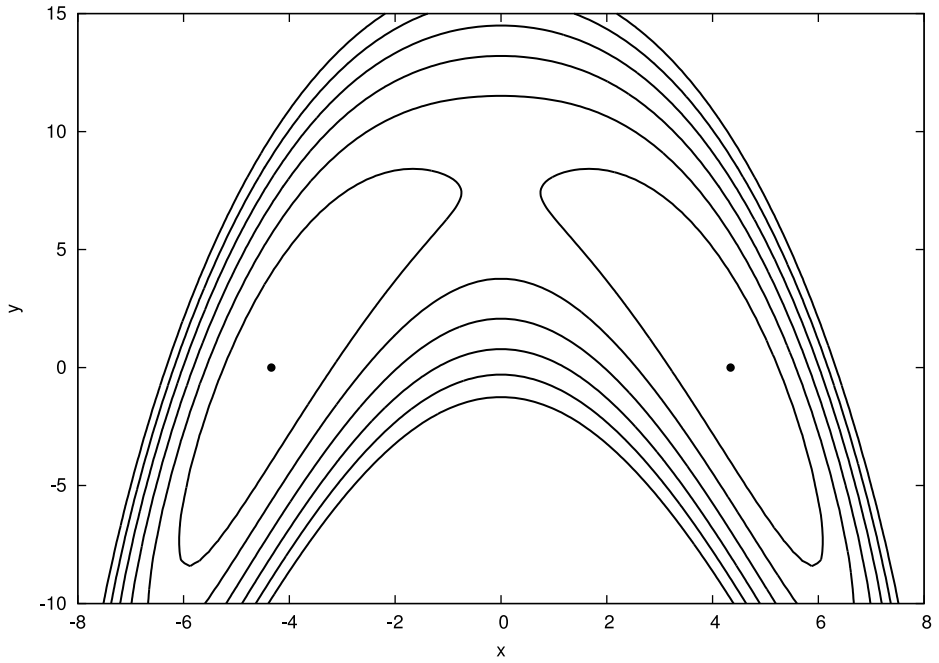

Figure 2.2: Contour plot of the potential $V(x,y)$ for $(R = 4.34, \omega = 1/4, \gamma = 0.47)$. The dots represent the minima of the potential.

Two wells of the potential appear to support doubly-degenerate bound states, but the degeneracy is lifted due to the tunneling. The splitting of the energy levels is illustrated in Fig. 2.3.

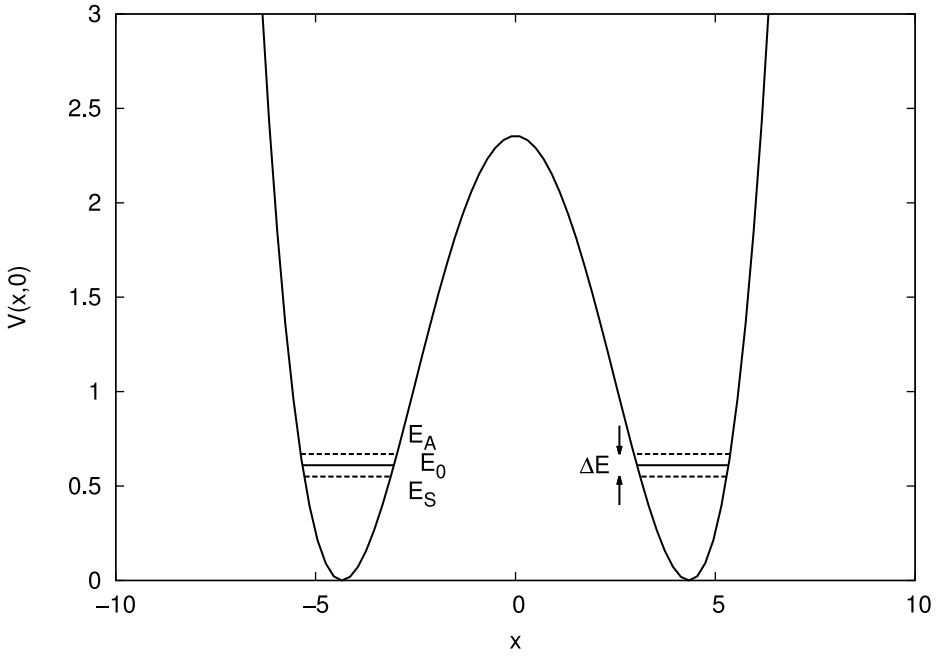

Figure 2.3: Plot of the $y = 0$ cut of the potential $V(x, y)$ for $R = 4.34$.

The function Ψ_S of the state with lower energy E_S is symmetric with respect to the reflection around y-axis and the wave fuction Ψ_A of the state with higher energy E_A is antisymmetric. The energy splitting is then defined as

$$\Delta E = E_A - E_S. \tag{2.2}$$

In the following, we consider the Hamiltonian of the problem in dimensionless units

$$\hat{H} = -\frac{1}{2}\frac{\partial^2}{\partial x^2} - \frac{1}{2}\frac{\partial^2}{\partial y^2} + V(x, y). \tag{2.3}$$

2.3.2 Parameters for malonaldehyde

We want to test our method for a set of parameters that are relevant for malonaldehyde. We take the parameters given by the fit of *ab initio* data from [37]. In that work, the electronic wave function was determined by Hartree-Fock self-consistent field calculations using the split valence basis set 3-21G. Geometry optimization and location of stationary points was found with the Schlegel gradient optimization algorithm.

Although *ab initio* data from newer and more accurate methods were published [51], we restrict ourselves to a simplified model. It suffices to yield the information about what subset of the parameters (R, ω, γ) is relevant in realistic calculation.

In [37] the potential is given in a form

$$V_B\left(x, y\right) = -a_B x^2 + b_B x^4 + \left(2\pi\nu_B\right)^2 \left[y - \frac{c_B x^2}{\left(2\pi\nu_B\right)^2}\right]^2, \tag{2.4}$$

where Cartesian coordinates x and y are mass-weighted, i.e. in units of $\sqrt{\mathrm{m}_u}$Å. The parameters of (2.4) have values

$$a_B = 42.0\,\mathrm{kcal\,mol^{-1}\,\AA^{-2}\,m_u^{-1}}\,, \tag{2.5}$$

$$b_B = 88.5\,\mathrm{kcal\,mol^{-1}\,\AA^{-4}\,m_u^{-2}}\,, \tag{2.6}$$

$$c_B = 0.93\,\mathrm{mdyn\,\AA^{-2}\,m_u^{-3/2}}\,, \tag{2.7}$$

$$\nu_B = 675\,\mathrm{cm^{-1}}\,. \tag{2.8}$$

It is necessery to mention that parameter c_B (2.7) is given in wrong units in the article [37]. We need to find a transformation $(a_B, b_B, c_B, \nu_B) \to (R, \omega, \gamma)$. The transformation is not entirely trivial; therefore, we describe it here in detail. Firstly, we write the Schrödinger equation in both units and expand the parentheses. We get

$$\left[-\frac{1}{2}\frac{\partial^2}{\partial x^2} - \frac{1}{2}\frac{\partial^2}{\partial y^2} + \frac{x^4}{8R^2} - \frac{x^2}{4} + \frac{R^2}{8} + \frac{x^2}{R^2}\gamma y - \gamma y + \frac{\omega^2}{2}y^2\right]\Psi \;=\; E\Psi\,, \tag{2.9}$$

and

$$\left[-\frac{\hbar^2}{2}\frac{\partial^2}{\partial x^2} - \frac{\hbar^2}{2}\frac{\partial^2}{\partial y^2} - a_B x^2 + b_B x^4 + (2\pi\nu_B)^2 y^2 - c_B x^2 y + \frac{c_B^2 x^4}{(2\pi\nu_B)^2}\right]\Psi = \\ = E_B\Psi\,. \tag{2.10}$$

In order to find the relations between the parameters we need to modify both equations in an apropriate way. In the first equation we make a substitution $y \to y + \gamma/\omega^2$ and move constant terms to the right. In the second equation we first make a substitutions $y \to \xi y$, $x \to \xi x$, where ξ is the transformation parameter. Then we simplify the equation and rewrite parameters (a_B, b_B, c_B, ν_B) to the same units so we convert them all to SI units

$$a'_B = a_B\,\frac{\mathrm{J}}{\mathrm{kcal\,mol^{-1}}}\,\frac{\mathrm{m^2kg}}{\mathrm{\AA^2\,m_u}}\,, \tag{2.11}$$

$$b'_B = b_B\,\frac{\mathrm{J}}{\mathrm{kcal\,mol^{-1}}}\,\frac{\mathrm{m^2kg}}{\mathrm{\AA^2\,m_u}}\,, \tag{2.12}$$

$$c'_B = c_B\,\frac{\mathrm{N}}{\mathrm{mdyn}}\,\frac{\mathrm{m^3kg}}{\mathrm{\AA^3\,m_u}}\,, \tag{2.13}$$

$$\nu'_B = \nu_B c\,\frac{\mathrm{m^2kg}}{\mathrm{\AA^2\,m_u}}\,, \tag{2.14}$$

where c on the right-hand side (RHS) of the last equation is the speed of light. We thus have the equations in the form

$$\left[-\frac{1}{2}\frac{\partial^2}{\partial x^2} - \frac{1}{2}\frac{\partial^2}{\partial y^2} + \frac{1}{8R^2}x^4 + \left(-\frac{1}{4} + \frac{\gamma^2}{R^2\omega^2}\right)x^2 + \right. \\ \left. + \frac{\gamma}{R^2}x^2 y + \frac{\omega^2}{2}y^2\right]\Psi = \left[E - \frac{R^2}{8} + \frac{\gamma^2}{2\omega^2}\right]\Psi\,, \tag{2.15}$$

and

$$\left[-\frac{1}{2}\frac{\partial^2}{\partial x^2} - \frac{1}{2}\frac{\partial^2}{\partial y^2} + \frac{1}{\hbar^2}\left(b'_B + \frac{1}{2}\frac{c'^2_B}{(2\pi\nu'_B)^2} \right)\xi^6 x^4 - \frac{a'_B}{\hbar^2}\xi^4 x^2 - \right.$$
$$\left. - \frac{c'_B}{\hbar^2}\xi^5 x^2 y + \frac{(2\pi\nu'_B)^2}{\hbar^2}\xi^4 y^2 \right]\Psi = \frac{\xi^2}{\hbar^2}E_B\Psi\,. \quad (2.16)$$

Comparing coefficients between terms of the potential we get four equations for four variables. We solve those equations and taking real positive solutions we get $(R = 4.34, \omega = 0.252, \gamma = 0.465, \xi = 0.112)$. For simplicity, we will use $(R = 4.34,\ \omega = 1/4,\ \gamma = 0.47)$.

The same procedure can be performed for parameters of the hydroxalate anion from [37] and for them we get $(R = 4.78, \gamma = 0.64, \omega = 0.32)$.

2.3.3 Variational calculation

Let us find the energies of the symmetric (S) and antisymmetric (A) states by means of the Ritz variational method [31],

$$E^{var}_{\substack{S\\A}} = \frac{\langle \Phi_{\substack{S\\A}} | \hat{H} | \Phi_{\substack{S\\A}} \rangle}{\langle \Phi_{\substack{S\\A}} | \Phi_{\substack{S\\A}} \rangle}. \quad (2.17)$$

The test functions $\Phi_{\substack{S\\A}}$ are taken as linear combinations

$$\Phi_{\substack{S\\A}} = \sum_{i=0}^{K}\sum_{j=0}^{L} c_{ij}\phi^{ij}_{\substack{S\\A}}\,. \quad (2.18)$$

of the symmetry adapted basis

$$\phi^{ij}_{\substack{S\\A}} = \psi_i(y;\omega) \times \begin{cases} [\psi_j(x-R;1) \pm \psi_j(x+R;1)] & \text{if } j \text{ is even} \\ [\psi_j(x-R;1) \mp \psi_j(x+R;1)] & \text{if } j \text{ is odd} \end{cases}\,. \quad (2.19)$$

The functions $\psi_n(x;\Omega)$ are wave functions of the harmonic oscilator with frequency Ω,

$$\psi_n(x;\Omega) = \sqrt[4]{\frac{\Omega}{\pi}}\frac{1}{\sqrt{n!\,2^n}}H_n(\sqrt{\Omega}x)\mathrm{e}^{-\Omega x^2}\,, \quad (2.20)$$

where $H_n(x)$ is Hermite polynomial defined as

$$H_n(x) = (-1)^n \mathrm{e}^{x^2}\frac{\mathrm{d}^n}{\mathrm{d}x^n}\mathrm{e}^{-x^2}. \quad (2.21)$$

More information about Hermite polynomials can be found in [41], Apendix H. Since we use a linear parametrization of the basis (2.18), the problem is reduced to the generalized eigenvalue problem [31],

$$\mathsf{Hc} = \mathsf{Sc}, \quad (2.22)$$

where H resp. S are Hamiltonian and overlap matrices, respectively, and c are linear parameters defined in (2.18).

At this point, we only need to calculate the matrix elements in the basis $\phi^{ij}_{\substack{S\\A}}$ (2.19). To do it, we use several relations

$$\frac{1}{2}\left(-\frac{\mathrm{d}^2}{\mathrm{d}x^2}+\Omega^2x^2\right)\psi_n(x;\Omega)=\Omega\left(n+\frac{1}{2}\right)\psi_n(x;\Omega)\,, \tag{2.23}$$

$$x\psi_n(x;\Omega)=\frac{1}{\sqrt{2\Omega}}\left(\sqrt{n+1}\psi_{n+1}(x;\Omega)+\sqrt{n}\psi_{n-1}(x;\Omega)\right)\,, \tag{2.24}$$

$$\int_{-\infty}^{\infty}\mathrm{d}x\,\psi_n(x;\Omega)\psi_m(x;\Omega)=\delta_{nm}\,. \tag{2.25}$$

The derivation of these relations is trivial and a part of many basic textbooks [41, 31]. The features of Hermite polynomials also provide us with tools to calculate a nontrivial "overlap" integral O_{nm} between functions $\psi_n(x-R;1)$ and $\psi_m(x+R;1)$

$$\begin{aligned}O_{nm}&=\int_{-\infty}^{\infty}\mathrm{d}x\,\psi_n(x-R;1)\psi_m(x+R;1)=\\&=\frac{1}{\sqrt{\pi}}\frac{\mathrm{e}^{-R^2}}{\sqrt{n!\,m!\,2^{n+m}}}\int_{-\infty}^{\infty}\mathrm{d}x\,\mathrm{e}^{-x^2}H_n(x-R)H_m(x+R)\end{aligned} \tag{2.26}$$

We use a procedure described in [41] Apendix H. It uses the so called *generating function*

$$S(x,\xi)=\mathrm{e}^{x^2-(\xi-x)^2}, \tag{2.27}$$

which is substituted for the Hermite polynomial $H_n(x)\to S(x,\xi)$ and then the integral of the gaussian type is calculated. The original integral is retrieved by making use of the relation

$$H_n(x)=\left.\frac{\mathrm{d}^nS(x,\xi)}{\mathrm{d}\xi^n}\right|_{\xi=0}. \tag{2.28}$$

Following the outlined procedure we calculate the integral

$$\begin{aligned}I(\xi,\rho;R)&=\int_{-\infty}^{\infty}\mathrm{d}x\,\mathrm{e}^{-x^2}S(x-R,\xi)S(x+R,\rho)=\\&=\int_{-\infty}^{\infty}\mathrm{d}x\,\mathrm{e}^{-(x-\xi-\rho)^2+2\xi\rho+2R(\rho-\xi)}=\sqrt{\pi}\mathrm{e}^{2\xi\rho+2R(\rho-\xi)}\end{aligned} \tag{2.29}$$

and we use it to find the formula for O_{nm} from (2.26)

$$\begin{aligned}O_{nm}&=\frac{1}{\sqrt{\pi}}\frac{\mathrm{e}^{-R^2}}{\sqrt{n!\,m!\,2^{n+m}}}\left.\frac{\partial^{n+m}}{\partial\xi^n\partial\rho^m}I(\xi,\rho;R)\right|_{\xi=0,\rho=0}=\\&=\frac{\sqrt{2^{n+m}}}{\sqrt{n!\,m!}}\mathrm{e}^{-R^2}\sum_{k=0}^{\mathrm{Min}(n,m)}\binom{n}{k}\binom{m}{k}\frac{(-1)^{n-k}k!}{2^k}R^{n+m-2k}.\end{aligned} \tag{2.30}$$

Using the just derived formula and (2.25) we get the overlap matrix elements $S_S^{ij,kl}$ between the basis functions in the form

$$S_S^{ij,kl}=\int_{-\infty}^{\infty}\mathrm{d}x\int_{-\infty}^{\infty}\mathrm{d}y\,\phi_S^{ij}\phi_S^{kl}=\delta_{ik}\cdot\begin{cases}2\delta_{jl}+2O_{jl} & \text{if } j \text{ and } l \text{ are both even}\\ -2O_{jl} & \text{if } j \text{ is even and } l \text{ is odd}\\ 2O_{jl} & \text{if } j \text{ is odd and } l \text{ is even}\\ 2\delta_{jl}-2O_{jl} & \text{if } j \text{ and } l \text{ are both odd}\end{cases} \tag{2.31}$$

The overlap matrix elements for the antisymmetric basis $S_A^{ij,kl}$ are computed in the same manner as $S_S^{ij,kl}$. The formula for $S_A^{ij,kl}$ is alike the (2.31) where only the cases for even indices j and l are changed for odd and vice versa.

Next we express matrix elements of Hamiltonian (2.3). It is done in the similar way, only before the use of (2.25) and (2.30) we apply the relations (2.23) and (2.24). We get

$$H_S^{ij,kl} = \int_{-\infty}^{\infty} \mathrm{d}x \int_{-\infty}^{\infty} \mathrm{d}y\, \phi_S^{ij} \hat{H} \phi_S^{kl} = \left[\omega\left(i+\frac{1}{2}\right) + \left(j+\frac{1}{2}\right)\right] S_S^{ij,kl} + \\ + \left(V_{4S}^{j,l} + V_{3S}^{j,l}\right)\delta_{ik} + \frac{\gamma}{\sqrt{\omega}}\left(V_{2S}^{j,l} + V_{1S}^{j,l}\right)\left(\sqrt{i+1}\delta_{i+1,k} + \sqrt{i}\delta_{i-1,k}\right) , \quad (2.32)$$

The first term comes from (2.23) and matrix elements $V_{nS}^{j,l}$ where n is between 1 and 4, and it is proportional to the power of the expression $(x \pm R)^n$. For example, it holds

$$V_{4S}^{j,l} = \frac{1}{8R^2}\int_{-\infty}^{\infty} \mathrm{d}x\, \left[\psi_j\left(x-R;1\right) \pm \psi_j\left(x-R;1\right)\right] \times \\ \times \left[(x-R)^4 \psi_l\left(x-R;1\right) \pm (x+R)^4 \psi_l\left(x+R;1\right)\right] , \quad (2.33)$$

where plus sign is taken if j, resp. l, is even, minus sign if j, resp. l, is odd. The expression is then calculated by using recurrence relation (2.24) four times[5] and after expansion of the brackets, all integrals are equal either to Kronecker deltas, cf. Eq. (2.25), or O_{jl} defined in (2.26). We do not give the full final expression here because it is widespread and nontransparent. Moreover, it can be obtained by a straightforward application of the just described steps. Matrix elements $V_{nS}^{j,l}$ for n between 1 and 3 are calculated in the same way.

The Hamiltonian matrix elements for the antisymmetric basis $H_A^{ij,kl}$ are again the same as in (2.32) but with interchanged signs in basis (2.18) for odd and even j and l.

We take both maximum numbers of basis functions K and L from equation (2.18) between 20 and 25, using the lowest eigenvalues we check the convergence and extrapolate them using Thielé-Padé method. For E_S and E_A we take the extrapolated values. Illustrating example is shown in Table 2.1.

max n, m	E_S	E_A	ΔE
20	0.527351236196450	0.533404148909829	0.00605291271338
21	0.527351230797662	0.533404148895860	0.00605291809820
22	0.527351229317104	0.533404148892978	0.00605291957587
23	0.527351228927321	0.533404148892405	0.00605291996508
24	0.527351228828652	0.533404148892295	0.00605292006364
25	0.527351228804598	0.533404148892276	0.00605292008768
ext	0.527351227872220	0.533404148890693	0.00605292101847

Table 2.1: Results for ($R = 4.34$, $\omega = 0.25$, $\gamma = 0.47$) rounded to 16 digits. In the last row are extrapolated results.

[5]For $V_{nS}^{j,l}$ it is used n-times.

2.3.4 Lifshitz-Herring formula

Another way to calculate the energy difference is by using the Lifshitz-Herring formula. For derivation in one-dimensional case see for example [17], chapter 7, &50, problem 3. Derivation of the formula for a general curved space is given in [46], Apendix C. Let us give here a derivation relevant to our case, i.e. in two-dimensional Euclidean space. We consider Schrödinger equation for anti-symmetric (A) and symmetric (S) states in natural units

$$\left[-\frac{\nabla^2}{2}+V\right]\underset{A}{\Psi}_{S}(x,y)=\underset{A}{E}_{S}\underset{A}{\Psi}_{S}(x,y) \tag{2.34}$$

Next we multiply the Schrödinger equation for state A by function Ψ_S and we subtract the Schrödinger equation for state S multiplied by function Ψ_A. We simplify it and get

$$\Delta E\,\Psi_A\Psi_S=-\Psi_S\frac{\nabla^2}{2}\Psi_A+\Psi_A\frac{\nabla^2}{2}\Psi_S=-\frac{\nabla}{2}\left(\Psi_S\nabla\Psi_A-\Psi_A\nabla\Psi_S\right)\,, \tag{2.35}$$

where ΔE is the sought energy splitting defined in (2.2). We now use several properties of our problem.

Firstly, we utilize the symmetry and we write the functions Ψ_S and Ψ_A using the symmetrical and asymmetrical combination of function Ψ that is the solution of the Schrödinger equation (2.34) restricted on a subspace $x \geq 0$. The functions Ψ_S and Ψ_A can be then defined via this function

$$\underset{A}{\Psi}_{S}(x,y)=\frac{1}{\sqrt{2}}\left[\Psi(x,y)\pm\Psi(-x,y)\right]. \tag{2.36}$$

Secondly, from the reflection symmetry around y it is also evident that:

$$\Psi_A(0,y)=0\,, \tag{2.37}$$

$$\left.\frac{\partial}{\partial x}\Psi(-x,y)\right|_{x=0}=-\left.\frac{\partial}{\partial x}\Psi(x,y)\right|_{x=0}\,. \tag{2.38}$$

Armed with the just introduced relations, we integrate the LHS of the equation (2.35) over x from 0 to ∞ and y over $-\infty$ to ∞ and we get

$$\Delta E\int_0^\infty \mathrm{d}x\int_{-\infty}^{\infty}\mathrm{d}y\,\Psi_A\Psi_S=\frac{\Delta E}{2}\int_0^\infty \mathrm{d}x\int_{-\infty}^{\infty}\mathrm{d}y\,\Psi^2(x,y)\,. \tag{2.39}$$

In the last simplification we have used the definitions of $\Psi(x,y)$ and $\underset{A}{\Psi}_{S}(x,y)$ (2.36). Then, we integrate in the same manner the RHS of the equation (2.35) using the Gauss's theorem[6] and we get

$$\begin{aligned}-\int_0^\infty \mathrm{d}x\int_{-\infty}^{\infty}\mathrm{d}y\,\frac{\nabla}{2}\left(\Psi_S\nabla\Psi_A-\Psi_A\nabla\Psi_S\right)=\\ =\frac{1}{2}\int_{-\infty}^{\infty}\mathrm{d}y\,\Psi_S(0,y)\left.\frac{\partial\Psi_A(x,y)}{\partial x}\right|_{x=0}=\\ =\frac{1}{2}\int_{-\infty}^{\infty}\mathrm{d}y\,\sqrt{2}\Psi(0,y)\left.\sqrt{2}\frac{\partial\Psi(x,y)}{\partial x}\right|_{x=0}\end{aligned} \tag{2.40}$$

[6] $\int_V \mathrm{d}V\nabla\cdot\mathbf{F}=\int_S\mathrm{d}\mathbf{S}\cdot\mathbf{F}$, where $\mathbf{S}=\partial V$

In the first equality we have used the feature (2.37) and the fact that the integrand is on the boundary nonzero[7] only for $x = 0$. In the second equality we have used the definition (2.36) and the feature (2.38).

Finally, we compare LHS (2.39) and RHS (2.40) and after trivial simplification we get the Lifshitz-Herring formula in the form

$$\Delta E = \frac{J}{N},$$
$$J = 2\int_{-\infty}^{\infty} \mathrm{d}y \Psi(0,y) \left.\frac{\partial \Psi(x,y)}{\partial x}\right|_{x=0}, \qquad N = \int_0^{\infty} \mathrm{d}x \int_{-\infty}^{\infty} \mathrm{d}y\, \Psi^2(x,y)\,. \quad (2.41)$$

We calculate the "probability current" J by means of the WKB method and the norm N by means of the RSP method.

Since we use different approaches to calculate the wave function Ψ in the nominator and denominator of (2.41), we have to assure that both wave functions have the same normalization. To guarantee it we use a method introduced in [53] which avoids the tedious procedure of explicit asymptotic matching. The method is based on the fact, cf. [53], that the asymptotic matching is automatically fulfilled if we normalize both wave functions in such a way that asymptotic expansion of their logarithm in the overlap region, i.e. a region where both aproximations hold, does not contain constant additive terms.

2.3.5 Calculation of N - RSP method

Firstly, we employ RSP method with expansion parameter $r = 1/R$ and we calculate norm

$$N = N^{(0)} + rN'^{(1)} + r^2 N'^{(2)} + \dots\,, \quad (2.42)$$

and energy

$$E = E^{(0)} + rE'^{(1)} + r^2 E'^{(2)} + \dots\,. \quad (2.43)$$

We move the coordinate system to the right well $x = R + q$ (we could perform the same calculation by choosing the left well $x = -R + q$). In variables q and y the Hamiltonian (2.3) has the form

$$\hat{H} = \underbrace{-\frac{1}{2}\frac{\partial^2}{\partial x^2} - \frac{1}{2}\frac{\partial^2}{\partial y^2} + \frac{q^2}{2} + \omega^2\frac{y^2}{2}}_{=H_0} + r\underbrace{\left(\frac{q^3}{2} + 2\gamma q y\right)}_{=V_1} + r^2\underbrace{\left(\frac{q^4}{8} + \gamma q^2 y\right)}_{=V_2}. \quad (2.44)$$

For $r \to 0\,(R \to \infty)$, both V_1 and V_2 vanish and H_0 is Hamiltonian of two independent harmonic oscilators for which there is an exact solution

$$E'^{(0)}_{nm} = m + \frac{1}{2} + \omega\left(n + \frac{1}{2}\right),$$
$$\langle q, y|\Psi^{(0)}_{nm}\rangle = \Psi^{(0)}_{nm}(q,y) = \psi_m(q;1)\psi_n(y;\omega)\,, \quad (2.45)$$

where functions of the harmonic oscilator $\psi_n(x;\Omega)$ were defined in (2.20). Results for the ground-state are given by the following well-known RSP recurrence

[7] We assume $\Psi \to 0$ for $x \to \infty$ and $y \to \pm\infty$. This is obvious because for large x and y potential goes to infinity.

relations

$$E'^{(0)} = E'^{(0)}_{00} = \frac{1+\omega}{2}, \tag{2.46}$$

$$|\Psi^{(0)}\rangle = C^{(0)}|\Psi^{(0)}_{00}\rangle, \tag{2.47}$$

$$E'^{(k)} = \frac{1}{(C^{(0)})^2}\Big[\langle\Psi^{(0)}_{00}|V_1|\Psi^{(k-1)}\rangle + \langle\Psi^{(0)}_{00}|V_2|\Psi^{(k-2)}\rangle - \sum_{l=1}^{k-1} E'^{(l)}\,\langle\Psi^{(0)}_{00}|\Psi^{(k-l)}\rangle\Big], \tag{2.48}$$

$$|\Psi^{(k)}\rangle = \sum_{n=0}^{k}\sum_{m=0}^{4k}|\Psi^{(0)}_{nm}\rangle\langle\Psi^{(0)}_{nm}|\Psi^{(k)}\rangle + C^{(k)}|\Psi^{(0)}_{00}\rangle, \tag{2.49}$$

$$\langle\Psi^{(0)}_{nm}|\Psi^{(k)}\rangle = \frac{1}{E'^{(0)}_{nm} - E'^{(0)}_{00}}\Big[-\langle\Psi^{(0)}_{nm}|V_1|\Psi^{(k-1)}\rangle - \langle\Psi^{(0)}_{nm}|V_2|\Psi^{(k-2)}\rangle + \sum_{l=1}^{k-1} E'^{(l)}\,\langle\Psi^{(0)}_{nm}|\Psi^{(k-l)}\rangle\Big]. \tag{2.50}$$

The constants $C^{(k)}$ are not given by the RSP method. We determine their values from the condition for the asymptotic matching that the logarithm of the wave function does not contain additive terms. This requirement is easily fulfilled if we take $\Psi^{(0)}(q,y) = \exp\{-\frac{q^2}{2} - \frac{\omega y^2}{2}\}$, i.e. $C^{(0)} = \sqrt[4]{\pi^2/\omega}$. In higher orders we take such $C^{(k)}$ that $\Psi^{(k)}(0,0) = 0$.

The norm is thus given by the formula

$$N'^{(k)} = \sum_{l=0}^{k}\langle\Psi^{(l)}|\Psi^{(k-l)}\rangle = \sum_{l=0}^{k}\sum_{n=0}^{\mathrm{Min}(l,k-l)}\sum_{m=0}^{4\cdot\mathrm{Min}(l,k-l)}\langle\Psi^{(l)}|\Psi^{(0)}_{nm}\rangle\langle\Psi^{(0)}_{nm}|\Psi^{(k-l)}\rangle \tag{2.51}$$

Using this scheme we can calculate norm and energy up to an arbitrary order because all the sums involved are finite. Therefore, $N'^{(k)}$ and $E'^{(k)}$ are polynomials in γ^2 of degree $k/2$.

Due to the symmetry of the Hamiltonian, for every odd order $2k+1$ it holds that energy and norm are zero[8], $E'^{(2k+1)} = 0$ and $N'^{(2k+1)} = 0$. We thus rewrite (2.42) and (2.43) to a form that is compatible with the following Sections

$$N = \sum_{j=0}^{\infty} r^{2j} N^{(j)}, \qquad N^{(j)} = N'^{(2j)} = \sum_{k=0}^{j} N^{(j)}_k \gamma^{2k}, \tag{2.52}$$

and

$$E = \sum_{j=0}^{\infty} r^{2j} E^{(j)}, \qquad E^{(j)} = E'^{(2j)}. \tag{2.53}$$

2.3.6 Calculation of J - WKB method

Let us turn to the problem of determination of the "probability current" J. The RSP method applies in the vicinity of the minimum of the potential. The magnitude of the wave function is the highest there, therefore it gives a good estimate of

[8]This does not hold for corrections to the wave function, i.e. $\Psi^{(1)} \neq 0$. However, the functions $\Psi^{(2k+1)}$ are needed only in an intermediate steps, for the calculation of energy splitting we only need the norm.

the norm. On the other hand, in the tunneling region where $q^2/2 \approx rq^3/2 + r^2q^4/8$, i.e. the perturbations $rV_1 + r^2V_2$ are of the same magnitude as H_0, the RSP method is not valid.

In order to describe the tunneling we turn to the WKB approximation. To make $q^2/2$, rV_1 and r^2V_2 of the same order in r we make a substitution $q = 2u/r$. The Schrödinger equation then has the form

$$\left[\frac{r^2}{4}\frac{\partial^2}{\partial u^2} + \frac{\partial^2}{\partial y^2}\right]\Psi = 2\left[\frac{2}{r^2}[u(u+1)]^2 + 4\gamma u(u+1)y + \frac{\omega^2}{2}y^2 - E\right]\Psi. \tag{2.54}$$

We search for a Ψ in the WKB form

$$\Psi_{\mathrm{WKB}}(u,y) = \mathrm{e}^{S(u,y)}, \tag{2.55}$$

where the action S is expanded in r^2 and y

$$S(u,y) = \sum_{j=-1}^{\infty}\sum_{i=0}^{2j+2} f_{i,j}(u) r^{(2j)}\frac{y^i}{i!}. \tag{2.56}$$

The structure of the differential equation (2.54) causes that the expansion in y is finite in every order of r^2. Inserting (2.55), (2.56) and (2.53) into (2.54) and comparing the same powers of y and r^2 we get, instead of partial differential equation (2.54), a series of ordinary differential equations. For r^{-2} order we have an equation that allows us to calculate $f_{0,-1}(u)$:

$$\left[f'_{0,-1}(u)\right]^2 = [u(u+1)]^2\,, \tag{2.57}$$

For r^0 we have equations that, if calculated gradually, provide us with the functions $f_{2,0}(u)$, $f_{1,0}(u)$, $f_{0,0}(u)$

$$f'_{0,-1}(u)f'_{2,0}(u) + f^2_{2,0}(u) = \omega^2, \tag{2.58}$$

$$2f'_{0,-1}(u)f'_{1,0}(u) + 2f_{2,0}(u)f_{1,0}(u) = 8\gamma u(u+1), \tag{2.59}$$

$$2f'_{0,-1}(u)f'_{0,0}(u) + f''_{0,-1}(u) + f^2_{1,0}(u) + f_{2,0}(u) = -2E^{(0)}, \tag{2.60}$$

and in higher orders we have

$$2f'_{0,-1}(u)f'_{4,1}(u) + 6\left[f'_{2,0}(u)\right]^2 + 8f_{2,0}(u)f_{4,1}(u) = 0\,, \tag{2.61}$$

$$\begin{aligned} 2f'_{0,-1}(u)f'_{3,1}(u) + 6f'_{1,0}(u)f'_{2,0}(u) + \\ +2f_{1,0}(u)f_{4,1}(u) + 6f_{2,0}(u)f_{3,1}(u) = 0\,, \end{aligned} \tag{2.62}$$

$$\begin{aligned} 2f'_{0,-1}(u)f'_{2,1}(u) + 2f'_{0,0}(u)f'_{2,0}(u) + f''_{2,0}(u) + \left[f'_{1,0}(u)\right]^2 + \\ +2f_{1,0}(u)f_{3,1}(u) + f_{4,1} + 4f_{2,0}(u)f_{2,1}(u) = 0\,, \end{aligned} \tag{2.63}$$

$$\begin{aligned} 2f'_{0,-1}(u)f'_{1,1}(u) + 2f'_{0,0}(u)f'_{1,0}(u) + f''_{1,0}(u) + \\ +2f_{1,0}(u)f_{2,1}(u) + f_{3,1} + 2f_{2,0}(u)f_{1,1}(u) = 0\,, \end{aligned} \tag{2.64}$$

$$2f'_{0,-1}(u)f'_{0,1}(u) + \left[f'_{0,0}(u)\right]^2 + f''_{0,0}(u) + 2f_{1,0}(u)f_{1,1}(u) + f_{2,1} = -2E^{(1)}. \tag{2.65}$$

The equation for any $f_{i,j}(u)$ contain only functions $f_{k,l}(u)$ where $l < j$ or if $l = j$ then $k > i$, in other words only functions calculated in previous steps. For example, from Eq. (2.62) we calculate function $f_{3,1}(u)$ but we need to solve Eq. (2.61)

before because we need function $f_{4,1}(u)$ together with functions calculated in lower orders of r^2.

The solutions of (2.57) and (2.58) are

$$f_{0,-1}(u) = \pm\left(\frac{u^2}{2} + \frac{u^3}{3}\right) + C_1\,, \tag{2.66}$$

$$f_{2,0}(u) = \pm\omega\,. \tag{2.67}$$

We find the correct branches from the requirement that in the limit $r \to 0$, the WKB wave function (2.55) in the lowest order matches the zeroth order perturbative solution

$$\psi_{\rm WKB} \approx \mathrm{e}^{\pm\frac{1}{r^2}\left(\frac{u^2}{2}+\frac{u^3}{3}\right)+\frac{C_1}{r^2}\pm\omega\frac{y^2}{2}} = \mathrm{e}^{\pm\left(\frac{q^2}{2}+r\frac{q^3}{3}\right)+\frac{C_1}{r^2}\pm\omega\frac{y^2}{2}}\,, \tag{2.68}$$

$$\psi^{(0)}_{\rm RSP} = \mathrm{e}^{-\frac{q^2}{2}-\omega\frac{y^2}{2}}\,. \tag{2.69}$$

From comparison of Eqs. (2.68) and (2.69) it is evident that $C_1 = 0$ and we take the minus signs in (2.66) and (2.67).

The equations (2.57) and (2.58) are the only two which are not linear and the correct branches have to be chosen from the comparison with the RSP wave function.

As mentioned before, we want to know the effect of quantum corrections, i.e. go beyond the zeroth order in r^2 and calculate functions $f_{i,j}$ with $j \geq 1$. We thus refine our method so the calculation is done with a simple procedure that can be easily implemented with the use of a symbolic programing language like *Mathematica*, *Maple*, etc.

Firstly, we introduce auxiliary functions φ, Φ and χ which are defined by the following equations

$$f_{2,0} = f'_{0,-1}(\ln\varphi)', \tag{2.70}$$

$$f_{1,0} = -f'_{0,-1}\varphi\Phi', \tag{2.71}$$

$$1 = -2f'_{0,-1}\varphi^2\chi'. \tag{2.72}$$

Secondly, we define new functions $\xi_{i,j}$ and $\eta_{i,j}$. The definitions and transformations $\xi_{i,j} \to f_{i,j}$, $f_{i,j} \to \eta_{i,j}$ are given in [56], Eq. (A2). Thirdly, we expand functions $f_{i,j}$ in powers of γ

$$f_{2i,j}(u) = \sum_{k=0}^{j+1-i} f_{2i,j,k}(u)\gamma^{2k}\,, \qquad f_{2i+1,j}(u) = \sum_{k=0}^{j+1-i} f_{2i+1,j,k}(u)\gamma^{2k+1}\,. \tag{2.73}$$

Fourthly, we rearrange the functions $f_{i,j}(u)$ into functions $S_{i,j}(u)$ for which it holds

$$S\left(u, y+\Delta\right) = \sum_{j=-1}^{\infty}\sum_{i=0}^{2j+2} S_{i,j}(u)y^i r^{2j}\,,$$

$$S_{2i,j}(u) = \sum_{k=0}^{j+1-i} S_{2i,j,k}(u)\gamma^{2k}\,, \quad S_{2i+1,j}(u) = \sum_{k=0}^{j+1-i} S_{2i+1,j,k}(u)\gamma^{2k+1}\,, \tag{2.74}$$

where Δ is given by the requirement

$$\left.\frac{\partial S(u,y+\Delta)}{\partial y}\right|_{y=0} = 0\,. \tag{2.75}$$

It gives us $S_{1,j}(u)=0$, $S_{0,-1}(u)=4f_{0,-1}(u)$, $S_{0,0}(u)=f_{0,0}(u)-\frac{f_{1,0}^2(u)}{2f_{2,0}(u)}$, $S_{2,0}(u)=\frac{f_{2,0}(u)}{2}$ and so on.

We insert the just derived relations and simplifications into the formula (2.41) for J,

$$\begin{aligned} J = r\int_{-\infty}^{\infty}\mathrm{d}y\,\mathrm{e}^{\left\{2S\left(u=-\frac{1}{2},y\right)\right\}}\left.\frac{\partial S(u,y)}{\partial u}\right|_{u=-\frac{1}{2}} = \\ = r\int_{-\infty}^{\infty}\mathrm{d}y\,\mathrm{e}^{\left\{2\sum_{i,j}f_{i,j}\frac{y^i}{i!}r^{2j}\right\}}\left(\sum_{i,j}f'_{i,j}\frac{y^i}{i!}r^{2j}\right) = \\ = r\int_{-\infty}^{\infty}\mathrm{d}y\,\mathrm{e}^{\left\{2\sum_{i,j}S_{i,j}y^i r^{2j}\right\}}\left(\sum_{i,j}S'_{i,j}y^i r^{2j}\right)\,. \end{aligned} \tag{2.76}$$

In the last equality we have made a substitution $y\to y+\Delta$. We have also used a notation

$$f_{i,j}=f_{i,j}\left(u=-\tfrac{1}{2}\right) \qquad \text{and} \quad f'_{i,j}=f'_{i,j}\left(u=-\tfrac{1}{2}\right)\,, \tag{2.77}$$

$$S_{i,j}=S_{i,j}\left(u=-\tfrac{1}{2}\right) \qquad \text{and} \quad S'_{i,j}=S'_{i,j}\left(u=-\tfrac{1}{2}\right)\,. \tag{2.78}$$

In the end we put everything together. We insert N from (2.52) supplemented with (2.51) and J from (2.76) with rearanged functions (2.74) into the formula for energy splitting (2.41). We then get

$$\begin{aligned} \Delta E = \frac{R\mathrm{e}^{2S_{0,-1}R^2+2\bar{S}_{0,0}}}{N^{(0)}}S'_{0,-1}\int_{-\infty}^{\infty}\mathrm{d}y\,\mathrm{e}^{2S_{2,0}y^2}\times \\ \times\left[1+\frac{2}{R^2}\left(S_{0,1}+S_{2,1}y^2+S_{4,1}y^4\right)+\dots\right]\times \\ \times\frac{\left[1+\frac{1}{S'_{0,-1}R^2}\left(S'_{0,0}+y^2S'_{2,0}\right)+\dots\right]}{1+\frac{N^{(1)}}{N^{(0)}R^2}+\dots}\,, \end{aligned} \tag{2.79}$$

where just the integration over y has to be performed and we have again used the parameter $R=1/r$. We expand (2.79) in R^{-2} and then the integration over y is easily done since in every order of R^{-2} we have only gaussian integrals.

The final expression then has the form

$$\Delta E = \frac{R}{\sqrt{\pi}}\mathrm{e}^{-\frac{2R^2}{3}+g_0}\left(1+\frac{g_1}{R^2}+\frac{g_2}{R^4}+\dots\right)\,, \tag{2.80}$$

where coefficients g_j depend on γ and ω. Unfortunately, it is complicated to keep both parameters general throughout the whole calculation so we show the results in the article [56] for $\omega=1/4$.

2.3.7 Description of the method

Let us give here the concise recapitulation of the energy splitting calculation. The method is based on an introduction of functions $f_{i,j}(u)$ in (2.56). Firstly, we calculate the energy E (2.53) and norm N (2.52) by means of RSP method. Secondly, we calculate "probability current" J. We transform the partial differential equation (2.54) to the series of coupled ordinary differential equations of the first order (2.57)–(2.65) for $f_{i,j}(u)$. After that we employ transformations $\xi_{i,j} \to f_{i,j}$, $f_{i,j} \to \eta_{i,j}$ to reduce the problem of solving inhomogeneous differential equations to the direct integration. In the actual calculation we start with functions $f_{0,-1}$, $f_{2,0}$, $f_{1,0}$ and $f_{0,0}$ which are calculated from equations (2.57) – (2.60). Then we repeat the following steps for ascending j:

1. For all i from $2j+2$ down to 0:

   (a) We find $\xi'_{i,j}(u)$ from equation as a function of u through the relations $\xi'_{i,j} = \xi'_{i,j}(\eta_{i,j})$ and $\eta_{i,j} = \eta_{i,j}(f_{k,l})$, where $f_{k,l}(u)$ were determined in the previous steps.

   (b) We integrate $\xi'_{i,j}(u)$ with the condition $\xi_{i,j}(0) = 0$ if $i > 0$.

   (c) Through the relation $f_{i,j} = f_{i,j}(\xi_{i,j})$ we find $f_{i,j}(u)$.

2. For $f_{0,j}(u)$ we require that for $u \to 0$, $f_{0,j}(u) \to 0$. This ensures the correct asymptotic matching.

3. We find Δ (2.75) and rearrange the functions $f_{i,j}$ into $S_{i,j}$ and $f'_{i,j}$ into $S'_{i,j}$ (2.74).

4. We integrate over y and with the RSP calculated norm N we determine the value of g_j.

Finally, we put everything together and we determine the energy splitting ΔE from the equation (2.80).

2.3.8 Strong coupling

The series (2.80) is impractical if we want to describe the tunneling in malonaldehyde with parameters ($R = 4.34$, $\omega = 1/4$, $\gamma = 0.47$). To overcome this inconvenience we consider a "strong coupling expansion", i.e. instead of γ we use $\bar{\gamma} = \gamma/R$ and we keep this ratio fixed. Fortunately, we do not have to start from the beginning, we just need to reorder the terms in the series (2.74) as follows

$$\sum_{j=-1}^{\infty}\sum_{k=0}^{j+1-i} S_{i,j,k}(u)\frac{\gamma^{2k}}{R^{2j}} = \sum_{j=-1}^{\infty}\sum_{k=0}^{j+1-i} S_{i,j,k}(u)\frac{\bar{\gamma}^{2k}}{R^{2(j-k)}} = \\ = \sum_{j=-1}^{\infty}\sum_{k=0}^{\infty} S_{i,j+k,k}(u)\frac{\bar{\gamma}^{2k}}{R^{2j}} = \sum_{j=-1}^{\infty}\sum_{k=0}^{\infty} \bar{S}_{i,j,k}(u)\frac{\bar{\gamma}^{2k}}{R^{2j}}\,. \quad (2.81)$$

We thus rewrite the equation for the action (2.74) as

$$S\left(u, y+\Delta\right) = \sum_{j=-1}^{\infty} \sum_{i=0}^{2j+2} \bar{S}_{i,j}(u) y^i r^{2j}\,,$$
$$\bar{S}_{2i,j}(u) = \sum_{k=0}^{\infty} S_{2i,j+k,k}(u)\bar{\gamma}^{2k}\,, \quad \bar{S}_{2i+1,j}(u) = \sum_{k=0}^{\infty} S_{2i+1,j+k,k}(u)\bar{\gamma}^{2k+1}\,. \quad (2.82)$$

In a similar way we reorder the norm

$$N = \sum_{j=0}^{\infty} \bar{N}^{(j)} r^{2j}\,, \quad \bar{N}^{(j)} = \sum_{k=0}^{\infty} N_k^{(j+k)} \bar{\gamma}^{2k}. \quad (2.83)$$

Using the reordered series (2.82) and (2.83) and parameter R we get for the energy splitting

$$\Delta E = R\frac{\mathrm{e}^{2R^2\bar{S}_{0,-1}+2\bar{S}_{0,0}}}{\bar{N}_0}\bar{S}'_{0,-1}\int_{-\infty}^{\infty}\mathrm{d}y\mathrm{e}^{2\bar{S}_{2,0}y^2}\times$$
$$\left(1+\frac{2}{R^2}\left(\bar{S}_{0,1}+\bar{S}_{2,1}y^2+\bar{S}_{4,1}y^4\right)+\ldots\right)\frac{1+\frac{\bar{S}'_{0,0}+y^2\bar{S}'_{2,0}}{\bar{S}'_{0,-1}R^2}+\ldots}{1+\frac{\bar{N}^{(1)}}{\bar{N}^{(0)}R^2}+\ldots}\,, \quad (2.84)$$

where again $\bar{S}_{i,j} = \bar{S}_{i,j}(u=-1/2)$. The complication is that $\bar{S}_{i,j}$ and $\bar{N}^{(j)}$ are infinite series in $\bar{\gamma}^2$, unlike $S_{i,j}$ and $N^{(j)}$ which are finite series in γ^2.

We have analysed these infinite series using the method suggested in [55]. The analysis is comprehensively described in [56] and here we present only the results.

2.4 Results and discussion

Detailed presentation and discussion of the achieved results can be found in [56]. Let us give here a shorter summary of the most important results and qualitatively discuss the key points.

2.4.1 Weak coupling

The WKB method works better for higher values of ω and R (smaller r). This is to be expected since for the potentials with higher R the expansion (2.56) converges faster and for higher ω the potential is more harmonic and the leading order approximation is more valid.

The case with parameter γ is more complicated. The method works the best for $\gamma \approx \gamma_1$ where γ_1 is a special value of γ for which the coefficient g_1 from (2.80) is zero. For $\gamma < \gamma_1$ the smaller the γ is, the performance of the method is worse. This is certainly unexpected. The method works better for a special curvature ($\gamma = \gamma_1$) than for a corresponding one-dimensional tunneling $\gamma = 0$.

For $\gamma > \gamma_1$ the behavior is even more complicated. With higher γ the method not only works worse, but lower order corrections can even worsen the leading order estimate. From this feature it is evident that for malonaldehyde, we would need to calculate much more than 10 orders to get quantitative results and that is impractical.

$\bar{\gamma}$	0	1	var.	var. [cm^{-1}]
0.1	0.001595 (19.8)	0.001367(2.3)	0.00133183	3.57
0.107	0.005709 (26.3)	0.00475 (4.9)	0.00451869	12.1
0.11	0.01235 (33.3)	0.0101 (9.2)	0.00926990	24.8
0.1	0.00002587 (10.6)	0.00002358 (0.6)	0.0000233927	0.778
0.13	0.0004067 (17.9)	0.0003527(1.6)	0.000344889	1.43
0.134	0.0007611 (20.5)	0.000650 (2.1)	0.000631647	1.76

Table 2.2: The ground state tunneling splitting for the proton tunneling in malonaldehyde ($\omega = 0.25$, $R = 4.34$) and hydroxalate anion ($\omega = 0.32$, $R = 4.78$) in the upper and lower parts of the Table, respectively. The numbers 0 and 1 stand for evaluating the splitting with accuracy up to R^0 and to R^{-2}, respectively. The number in the paranthesis is the relative percentage error with respect to the variational result.

This behavior of the series (2.80) is not encountered in the one-dimensional case [57]. We conclude that it is a consequence of a competition between the positive corrections due to the curvature of the classical trajectory, on one hand, and negative corrections due to the quantum nature of motion, on the other one.

2.4.2 Strong coupling

From the numerical analysis of the infinite series $\bar{S}_{i,j}$ (2.82) and $\bar{N}^{(j)}$ (2.83) we have found a formula that is valid for $\bar{\gamma}$ approaching $\bar{\gamma}_s$ from below and sufficiently large R

$$\Delta E = K(R,\bar{\gamma}_s)\left(1-(\bar{\gamma}/\bar{\gamma}_s)^2\right)^{1/4}\times \\ \times\exp\{2R^2a_{-1}\left(1-(\bar{\gamma}/\bar{\gamma}_s)^2\right)^{1/2}+2a_0\left(1-(\bar{\gamma}/\bar{\gamma}_s)^2\right)^{-1/2}\}\,, \quad (2.85)$$

where $K=\sqrt{\omega/(2\pi)}R\bar{S}'_{0,-1}(\bar{\gamma}_s)\exp\{2R^2\bar{S}_{0,-1}(\bar{\gamma}_s)\}/\sqrt{-\bar{S}_{2,0}(\bar{\gamma}_s)}$. Coefficients a_{-1} and a_0 are taken from the numerical analysis of the series. For $\omega = 1/4$ they have values $a_{-1} \simeq -0.76(2)$ and $a_0 \simeq 1.47(3)$. Be aware that the formula (2.85) can be used only in the semiclassical region. For $\bar{\gamma}$ aproaching $\bar{\gamma}_s$ this means we have to go to very large R.

The equation (2.85) shows strong sensitivity of the energy splitting on the parameter $\bar{\gamma}$ near the point $\bar{\gamma}_s$. The expression $1/\sqrt{1-(\bar{\gamma}/\bar{\gamma}_s)^2}$ is extremely sensitive to slight variation of $\bar{\gamma}$ near $\bar{\gamma}_s$, even further it gets exponentiated.

In Tab. 2.2 the results given by Eq. (2.84) for the ground-state tunneling splitting for the values of the parameters modeling the proton transfer in malonaldehyde and hydroxalate anion are displayed and compared with variational calculation. The series for the functions $\bar{S}_{i,j}$ and their derivatives were accelerated, see Tab. V of [56].

The sensitivity shown in the equation (2.85) is backed up by the results given in Table 2.2. They show that parameters describing malonaldehyde are in a region where rounding errors dramatically change the energy splitting. This might explain the large span of the results for malonaldehyde given in the literature [36, 46, 47, 49]. Also the results in Table 2.2 demonstrate that ignoring the

quantum corrections might not be valid. For the potentials, where the $\bar{\gamma}$ is close to the $\bar{\gamma}_s$, the importance of quantum corrections is not negligible.

The comparison of the results in Tab. 2.2 for malonaldehyde and hydroxalate anion also show that our method works better for the latter one. The ratio $\bar{\gamma}/\bar{\gamma}_s$ that measures how close we are to the critical point is $\bar{\gamma}/\bar{\gamma}_s \approx 0.86$ for malonaldehyde and $\bar{\gamma}/\bar{\gamma}_s \approx 0.84$ for hydroxalate anion. We can thus conclude that the importance of quantum corrections grows with the growing ratio $\bar{\gamma}/\bar{\gamma}_s$, i.e. with the proximity of the critical point $\bar{\gamma}_s$.

The strong dependence of the energy splitting on the input parameters suggests manifestation of quantum chaos [50, 48]. The strong sensitivity originates from the "virtual" bound state at the point $x = 0$, $y = \gamma/\omega^2$.

Furthermore, these results clearly show that if multi-dimensional tunneling is reduced to one dimension[9], some essential aspects of the problem are ignored.

[9]This approach is used for example in [51].

Conclusion

The main results reported in this work are:

- We studied the vacuum polarization effect and derived an expression for the Laplace transform of the vacuum charge density that can be used to calculate the energy shift. We expanded it and obtained the formulae for the Uehling and Wichmann-Kroll potentials. We calculated the energy shift caused by the Wichmann-Kroll potential to the Lamb shift in muonic hydrogen. The results are the most precise and in good agreement compared with those given in literature.

- We also studied the two-photon correction where the self-energy effect was perturbed by the Uehling potential. We derived an expression for the calculation of the extended Bethe logarithm and we calculated the energy shift of the Lamb shift in muonic hydrogen caused by it. Our result is more accurate and slightly different from those given before, but the change does not explain the "proton radius puzzle".

- Further, we suggested a new WKB method for calculating energy splitting due to tunneling in a non-separable multi-dimensional potential. Additionally, this method provided us with quantum corrections to the semi-classical results. We also observed quantum chaos as a strong sensitivity of the energy splitting to the slight variations of the input parameters. We concluded that although the WKB methods of Milnikov *et al.* [46, 47] or Richardson *et al.* [49] give qualitatively good results, it is necessary to supplement them with very accurate parameters of the potential energy surface. Moreover, we showed that the quantum corrections are needed for the results to be reliable.

Possible continuation of our work is following:

- It is possible to go further and calculate relativistic corrections to the Wichmann-Kroll potential or take the following term of the expansion of $q(b)$ (1.40) that is of the order $\alpha(Z\alpha)^8$. The same procedure can be applied but at the current level of experiment it is not necessary.

- We can calculate the combined self-energy vacuum polarization effect to higher orders of the expansion. This would give only small corrections that are not needed now.

- We can study the effects of vacuum polarization insertion into the photon line and of double self-energy.

- We can try to generalize our method of calculating the energy splitting caused by tunneling and examine either excited states or three- and more-dimensional potentials.

- We can also try to find an independent derivation of the formula (2.85).

Bibliography

[1] Antognini, A., *et al.*, Science **339** (2013), 417.

[2] Antognini, A., *et al.*, EPJ Web of Conf. **113** (2016), 01006.

[3] Berestetskii V.B., *et al.*: *Quantum Electrodynamics*, 2nd Edition, Pergamon Press, Oxford, 1982.

[4] Bethe H. A., *et al.*, Phys. Rev. **77** (1950), 370.

[5] Biedenharn L. C., Phys. Rev. **126** (1962), 845.

[6] Blomqvist J., Nucl. Phys. B **48** (1972), 95.

[7] Borie E., Phys. Rev. A 71 (2005) 032508.

[8] Brown L. S., *et al.* , Phys. Rev. D **12**, 581 (1975), *ibid* **12**, 596 (1975).

[9] Eides M. I. *et al.*, Physics Reports **342** (2001), 63.

[10] Erdélyi A. ed., *Higher transcendetal functions Vol. I, Bateman manuscript project*, McGraw-Hill Book Company, Inc, New York, 1953.

[11] Greiner W., Reinhardt J.: *Quantum Electrodynamics*, Springer-Verlag, Berlin, 2003

[12] Jentschura U. D. and Mohr P. J., Phys. Rev. A **69** (2004), 064103.

[13] Jentschura U. D., Ann. Phys. **326** (2011), 500.

[14] Källén G., Sabry A., Dan. Mat. Fys. Medd. **29** (1955), 17.

[15] Karshenboim S. G., *et al.*, Phys. Rev. A **81** (2010), 060501.

[16] Karshenboim S. G., Phys. Rev. **D 90** (2014), 053012.

[17] Landau L.D., Lifschitz E.M., *Quantum Mechanics, Nonrelativistic Theory*, Pergamon Press, Oxford, 1968.

[18] Mohr P. J., Taylor B. N. and Newell B. D., Rev. Mod. Phys., **88** (2016), 1527.

[19] Parthey, *et al.*, Phys. Rev. Lett. **107** (2011), 203001.

[20] Patkóš V., Šimsa D. and Zamastil J., Phys. Rev. A **95** (2017), 012507.

[21] Pachucki K.., *et al.*, Phys. Rev. A **53** (1996), 2092.

[22] Pohl R., *et al.*, Nature (London) **466** (2010), 213.

[23] Pohl R., *et al.*, Science **353** (2016), no.6300, 669.

[24] Salpeter E. E. and Bethe H. A., Phys. Rev. **84** (1951), 1232.

[25] Sapirstein J. R., Yennie D. R., in T. Kinoshita (Ed.): *Quantum Electrodynamics*, World Scientific, Singapore, 1990.

[26] Schweber S. S.: *An Introduction to Relativistic Quantum Field Theory*, Harper & Row, New York, 1962

[27] Sick I., Prog. in Part. and Nuc. Phys. **67** (2012), 473.

[28] Soff G. and Mohr P. J., Phys. Rev. A **38** (1988), 5066.

[29] Uehling E. A., Phys. Rev. **48** (1935), 55

[30] Wichmann E. H. and Kroll N. M., Phys. Rev. **101** (1956), 843.

[31] Zamastil J. and Benda J.: *Kvantová mechanika a elektrodymanika*, Karolinum, Praha, 2016.

[32] Zamastil J., Ann. of Phys. **327** (2012), 297.

[33] Zamastil J. and Patkóš V., Phys. Rev. A **86** (2012), 042514.

[34] Zamastil J. and Patkóš V., Phys. Rev. A **88** (2013), 032501.

[35] Zamastil J. and Šimsa D., Ann. of Phys. **379** (2017), 131.

[36] Benderskij V. A., *et al.*, Phys. Rep. **233** (1993), 195; Benderskij V. A., *et al.*, Chem. Phys. **188** (1994), 19; Benderskij V. A., *et al.*, *ibid* **184** (1995), 1.

[37] Bosch E., *et al.*, J. Chem. Phys. **93** (1990), 5685.

[38] Coleman S., Phys. Rev. D **15** (1977), 2929.

[39] Creagh S. C., J. Phys. A **27** (1994), 4969; Creagh S.C. and Whelan N.D., Phys. Rev. Lett. **77** (1996), 4975; *ibid* **82** (1999), 5237.

[40] Firth D. W., *et al.*, J. Chem. Phys. **94** (1991), 1812; Baba T., *et al.*, J. Chem. Phys. **110** (1999), 4131.

[41] Formánek J.: *Úvod do kvantové teorie, Část I.*, Academia, Praha, 2004.

[42] Hammer T., *et al.*, J. Chem. Phys. **131** (2009), 224109.

[43] Huang Z. H., *et al.*, Phys. Rev. A **41** (1990), 32.

[44] Iwamoto A. and Tomita Y., Prog. Theor. Phys. **87** (1992), 1171.

[45] Marchi M. and Chandler D., J. Chem. Phys. **95** (1991), 889.

[46] Milnikov G. V. and Nakamura H., J. Chem. Phys. **115** (2001), 6881.

[47] Milnikov G. V. and Nakamura H., Phys. Chem. Chem. Phys. **10** (2008), 1374.

[48] Brodier O., *et al.*, Phys. Rev. Lett. **87** (2001), 064101, Ann. Phys. **300**, 88 (2002). See also Nöckel J. U. and Stone A. D., Nature **385** (1997), 45; Cao H. and Wiersig J., Rev. Mod. Phys. **87** (2015), 61; Mertig N., *et al.*, Phys. Rev. E **94** (2016), 062220.

[49] Richardson J. O. and Althorpe S. C., J. Chem. Phys. **134** (2011), 054109.

[50] Tomsovic S. and Ullmo D., Phys. Rev. E **50** (1994), 145.

[51] Wang Y., *et al.*, J. Chem. Phys. **128** (2008), 224314.

[52] Wang Y. and Bowman J. M., J. Chem. Phys. **129** (2008), 121103.

[53] Zamastil J., Čížek J. and Skála L., Phys. Rev. Lett. **84** (2000), 5683; Zamastil J., Čížek J. and Skála L., Phys. Rev. A **63** (2001), 022107.

[54] Zamastil J., Phys. Rev. A **72**, 024101 (2005).

[55] Zamastil J., *et al.*, Phys. Rev. A **81** (2010), 032118.

[56] Zamastil J. and Šimsa D., Phys. Rev. E **96** (2017), 062201.

[57] Zinn-Justin J. and U. D. Jentschura, Ann. Phys. **313** (2004), 197; *ibid* **313** (2004), 269;

Attachments

[35] Zamastil J. and Šimsa D., Ann. of Phys. **379** (2017), 131.
[20] Patkóš V., Šimsa D. and Zamastil J., Phys. Rev. A **95** (2017), 012507.
[56] Zamastil J. and Šimsa D., Phys. Rev. E **96** (2017), 062201.